

# PHOTONICS-BASED MACHINE LEARNING TO SPEED UP AND SIMPLIFY LABEL-FREE FLOW CYTOMETRY

Alessio Lugnan - 7 September 2021

Promotors: Peter Bienstman, Joni Dambre

# OUTLINE

## Introduction:

- Technique to improve: flow cytometry
- Approach: machine learning and neural networks
- Problem: microparticle classification algorithms limit the speed of flow cytometry
- Solution: a hardware-based machine learning approach

## White blood cell hologram classification

## Dimensionality expansion with dielectric scatterers

## Development of flow cytometry experiment

## Final experiment results

# INTRODUCTION

# A WORLD OF INTERESTING MICROPARTICLES

Liquids can host huge numbers and varieties of microscopic objects and life forms, for example:

- cells in blood
- microbes in water and food
- pollutants (e.g. microplastics) in water
- plankton in the ocean
- ...

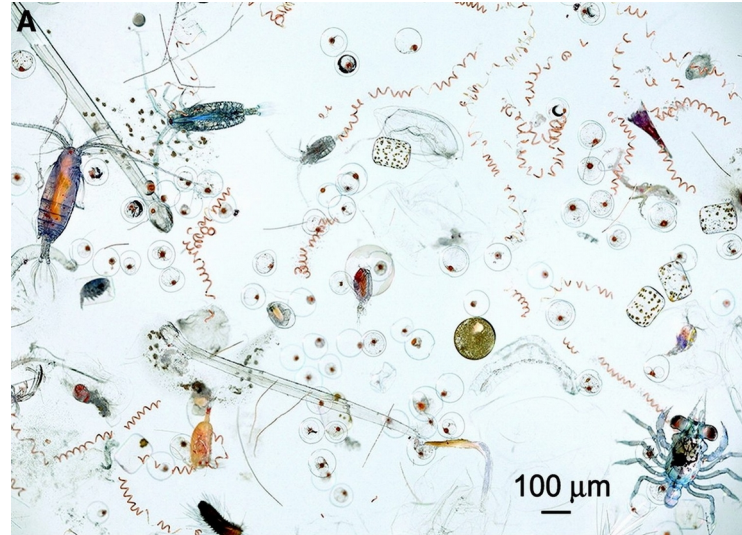


Images from Wikipedia.org

# NUMBERS MATTER

**Statistical validity** of scientific studies or **detection of rare objects** often require a large number of single-object measurements

→ **Flow cytometry** allows to analyse microscopic objects one by one, in a flow at high speed



Wikipedia.org



# NUMBERS MATTER

**Statistical validity** of scientific studies or **detection of rare objects** often require a large number of single-object measurements

→ **Flow cytometry** allows to analyse microscopic objects one by one, in a flow at high speed

Applications:

- Biological analysis of heterogeneous cell populations
- Cell sorting, to automatically isolate specific cell types
- Detection of circulating tumor cells in blood
- Blood analysis to monitor immune status
- Monitoring of waterborne microbes for water treatment and reuse
- Bacteria viability in probiotic products
- ...



Wikipedia.org



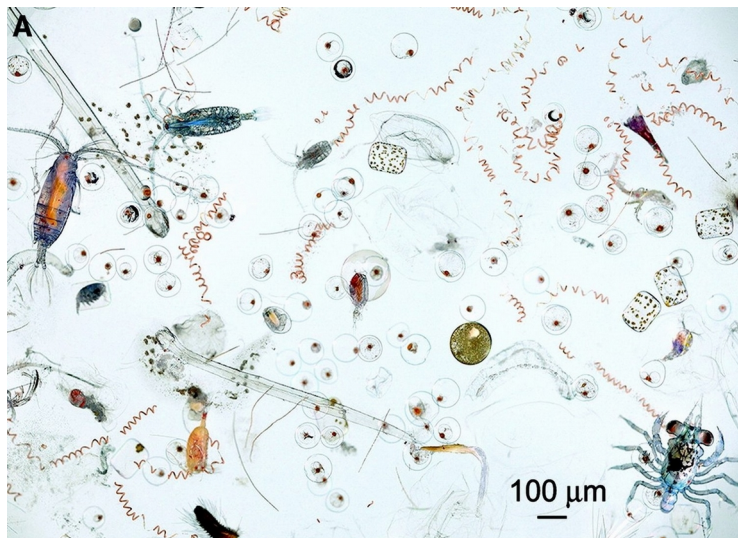
# NUMBERS MATTER

**Statistical validity** of scientific studies or **detection of rare objects** often require a large number of single-object measurements

→ **Flow cytometry** allows to analyse microscopic objects one by one, in a flow at high speed

Applications:

- Biological analysis of heterogeneous cell populations
- Cell sorting, to automatically isolate specific cell types
- Detection of circulating tumor cells in blood
- Blood analysis to monitor immune status
- Monitoring of waterborne microbes for water treatment and reuse
- Bacteria viability in probiotic products
- ...



Wikipedia.org



The related scientific community aims to make cytometers more compact, cheap, easy to use and fully automatic, to enable **versatile and in-situ implementations**

# POWERFUL AUTOMATIC ANALYSIS WITH MACHINE LEARNING

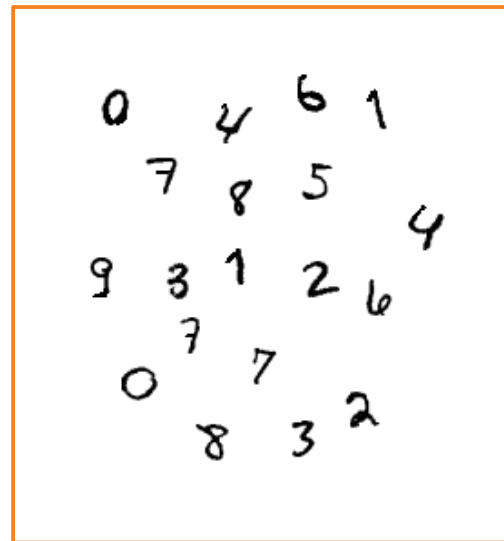
Machine learning (1959): algorithms learn to carry out a task through experience

Example task: written digits classification

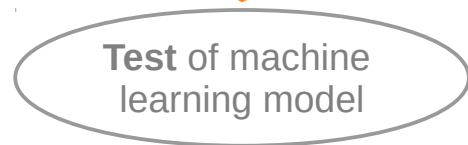
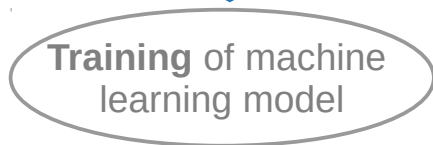
Class 1	0	0	0	0	0	0	0	0	0	0	0	0	0	0
Class 2	1	1	1	1	1	1	1	1	1	1	1	1	1	1
Class 3	2	2	2	2	2	2	2	2	2	2	2	2	2	2
Class 4	3	3	3	3	3	3	3	3	3	3	3	3	3	3
Class 5	4	4	4	4	4	4	4	4	4	4	4	4	4	4
Class 6	5	5	5	5	5	5	5	5	5	5	5	5	5	5
Class 7	6	6	6	6	6	6	6	6	6	6	6	6	6	6
Class 8	7	7	7	7	7	7	7	7	7	7	7	7	7	7
Class 9	8	8	8	8	8	8	8	8	8	8	8	8	8	8
Class 10	9	9	9	9	9	9	9	9	9	9	9	9	9	9

From MNIST dataset

Training samples

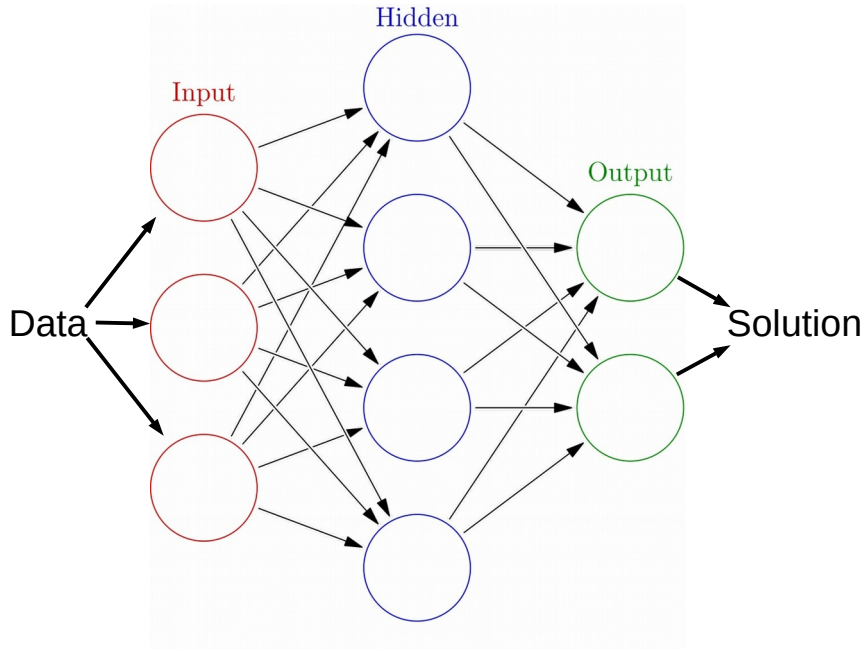
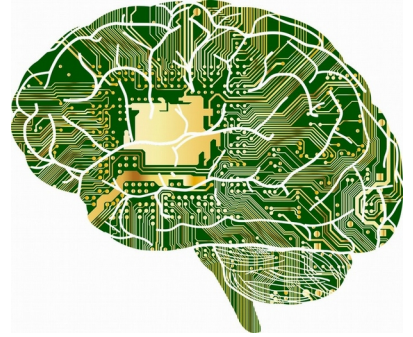


Test samples



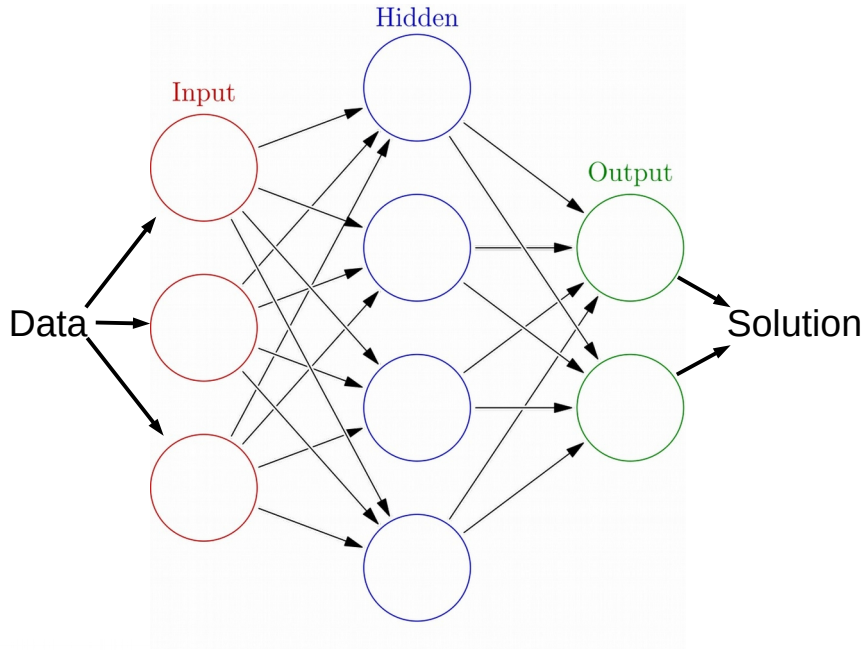
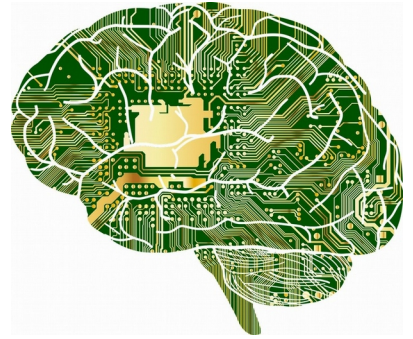
# INSPIRED BY THE BRAIN

**Neural network (NN)** models have grown more and more powerful in the past decade, **outperforming humans** in complex tasks such as image and speech recognition, lip reading, chess, etc...



# INSPIRED BY THE BRAIN

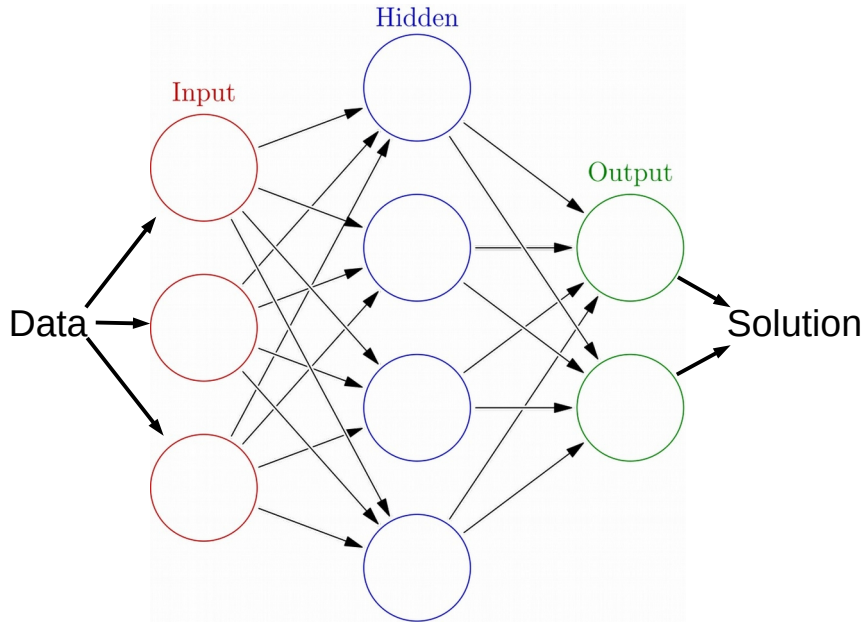
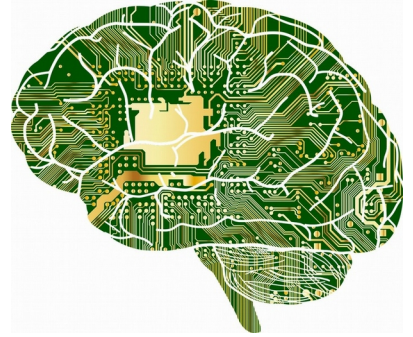
**Neural network (NN)** models have grown more and more powerful in the past decade, **outperforming humans** in complex tasks such as image and speech recognition, lip reading, chess, etc...



The larger the network, the higher the computational cost  
→ trade-off between speed, compactness and cost

# INSPIRED BY THE BRAIN

**Neural network (NN)** models have grown more and more powerful in the past decade, **outperforming humans** in complex tasks such as image and speech recognition, lip reading, chess, etc...



The larger the network, the higher the computational cost  
→ trade-off between speed, compactness and cost



**Hardware-based NNs can greatly improve efficiency and speed**

However they are usually difficult to train... we take a shortcut

# CONVENTIONAL FLOW CYTOMETRY

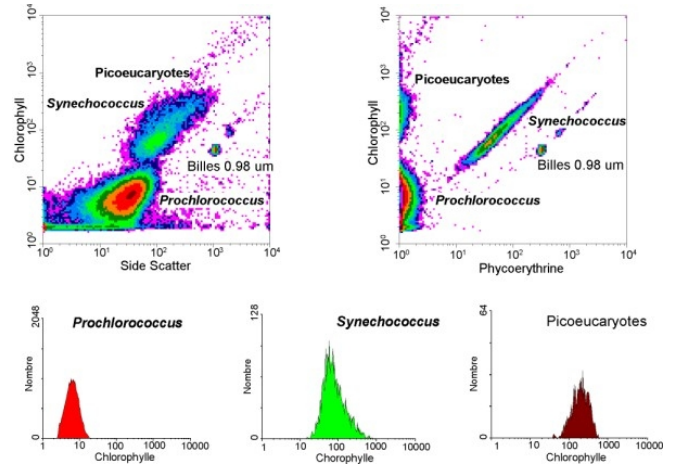
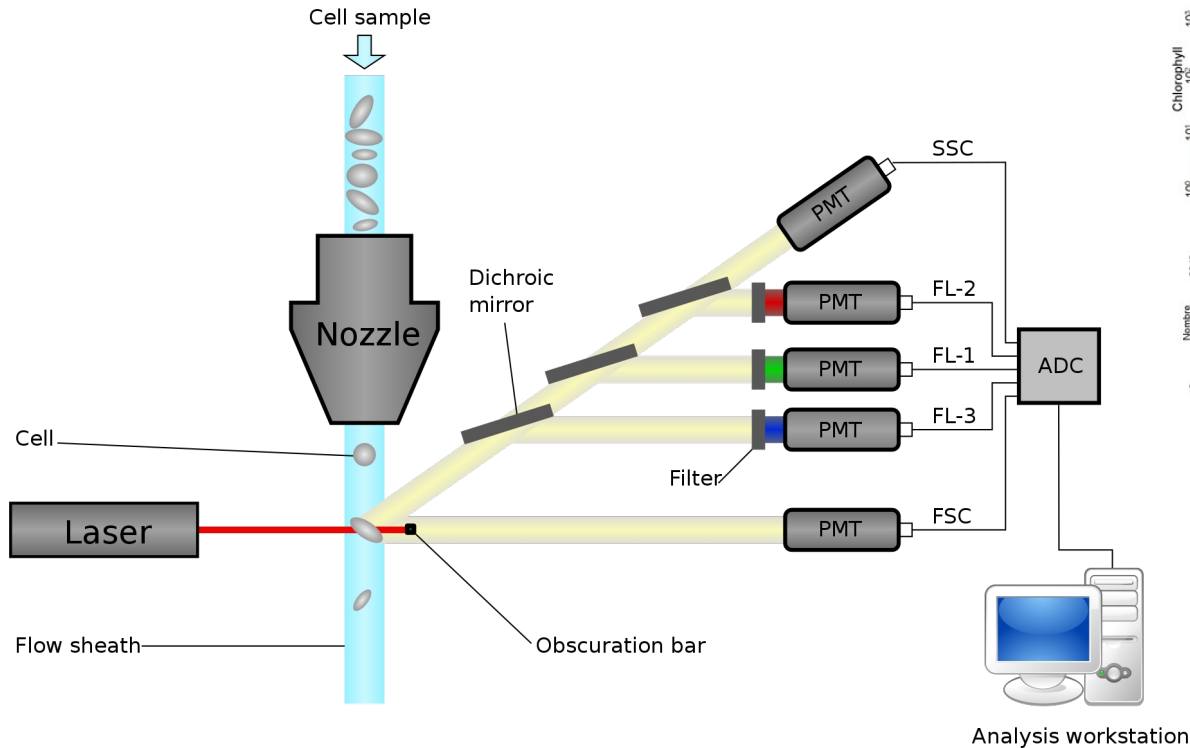


Image: [https://en.wikipedia.org/wiki/Flow\\_cytometry#/media/File:Picoplankton\\_cytometrie.jpg](https://en.wikipedia.org/wiki/Flow_cytometry#/media/File:Picoplankton_cytometrie.jpg)  
 License: <https://creativecommons.org/licenses/by-sa/2.5/deed.en>

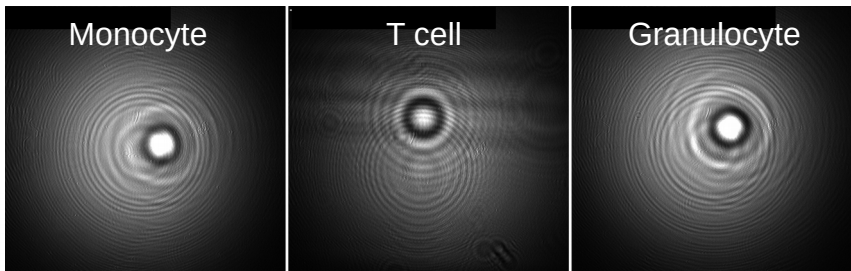
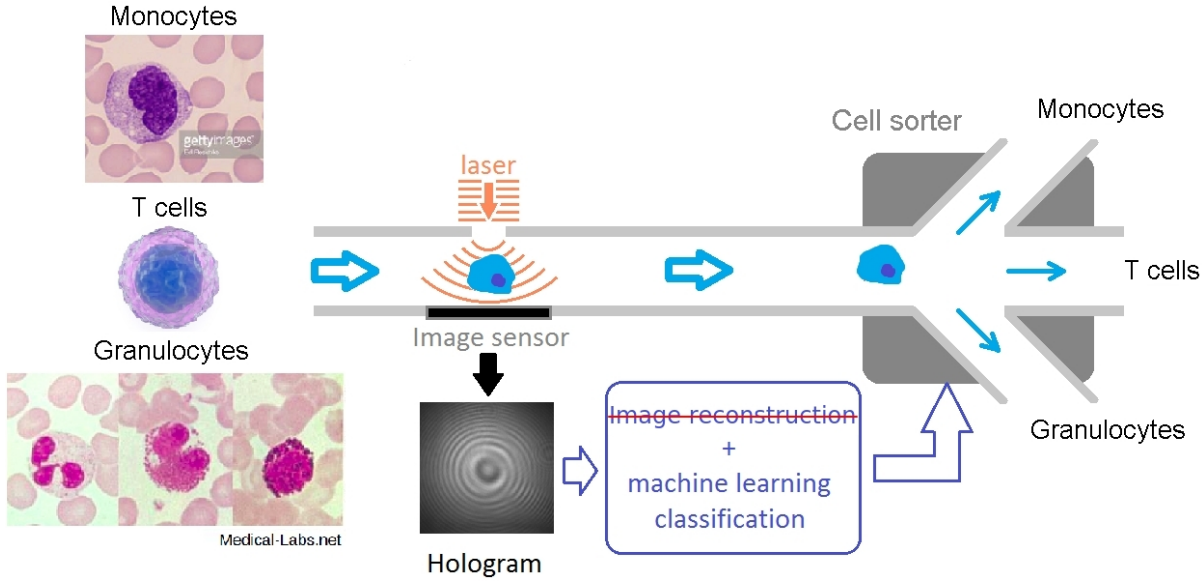
High throughput (~100,000 cell/s)

Fluorescent labels:

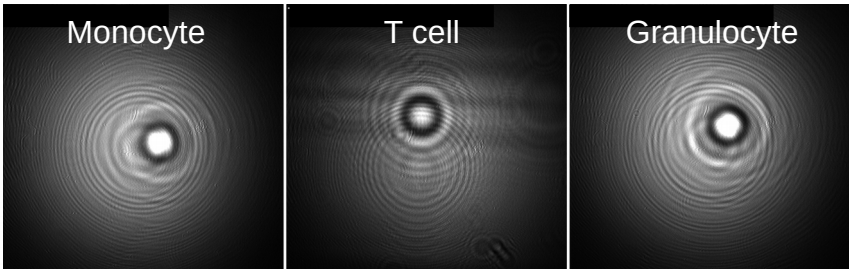
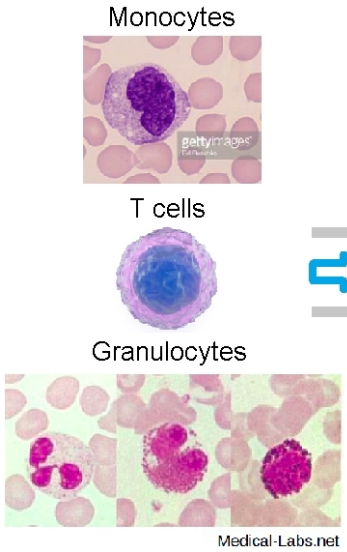
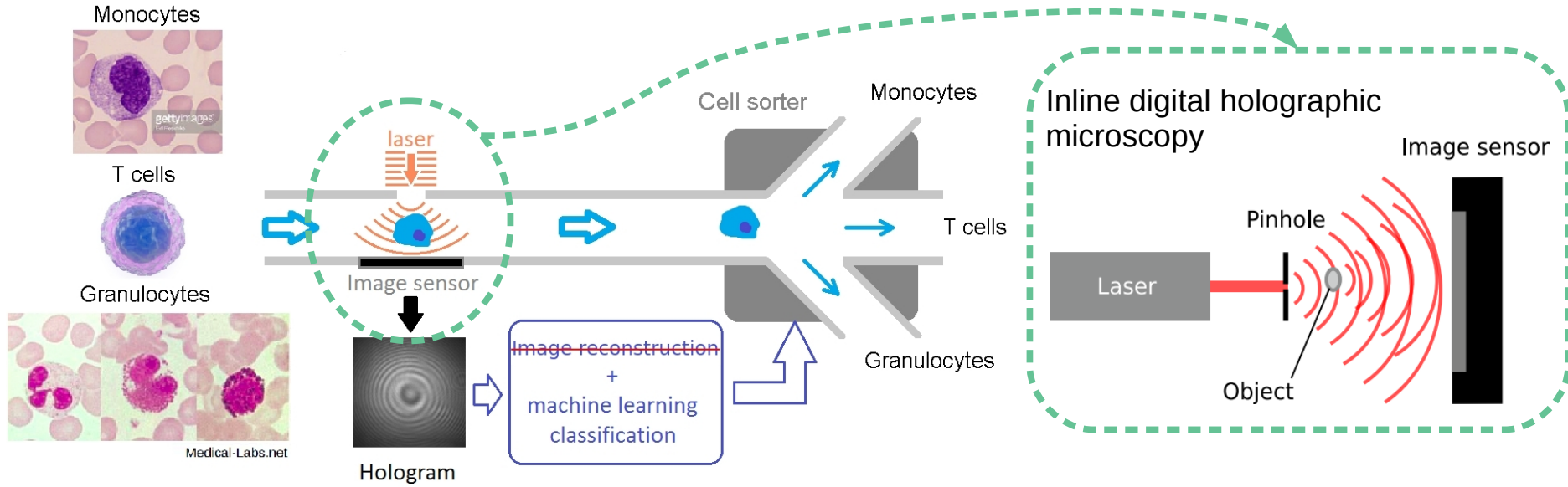
- often hinder live cell analysis
- additional cost and effort

Image: <https://commons.wikimedia.org/wiki/File:Cytometer.svg>  
 License: <https://creativecommons.org/licenses/by/3.0/deed.en>

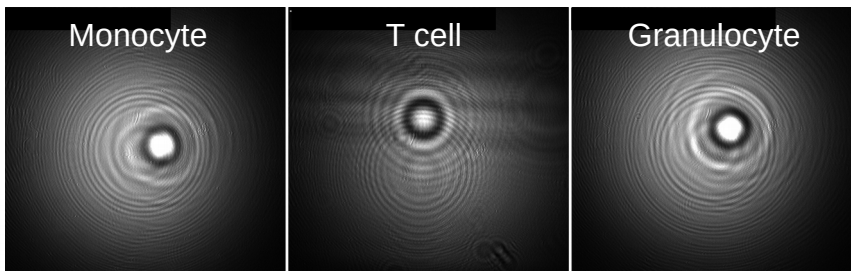
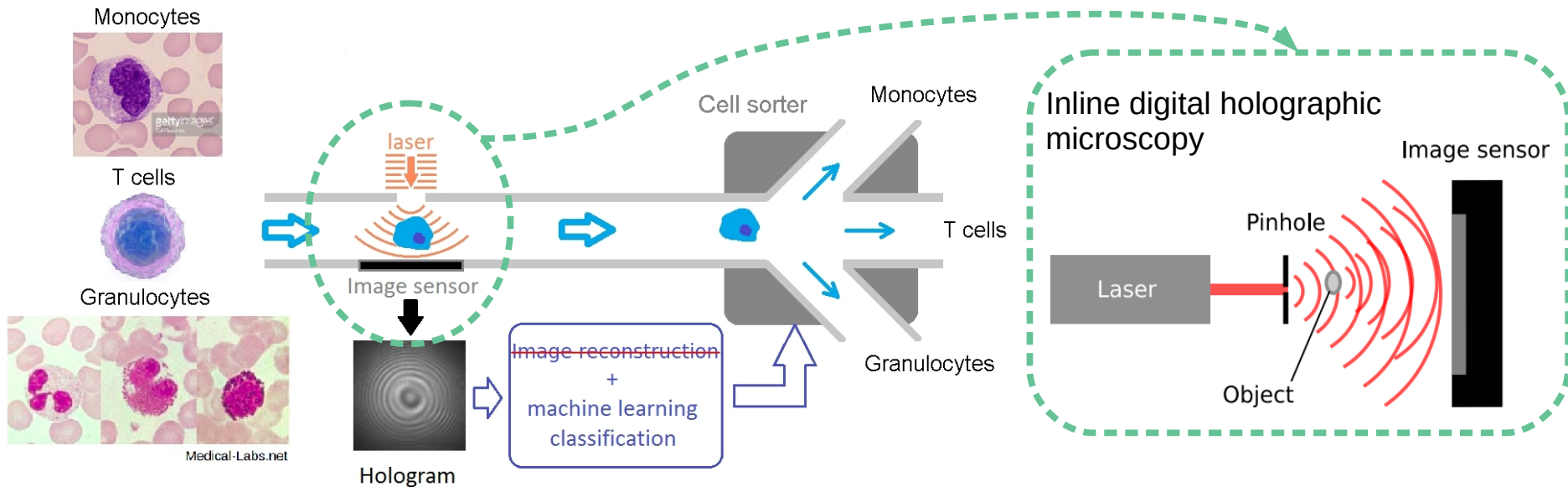
# LABEL-FREE IMAGING FLOW CYTOMETRY



# LABEL-FREE IMAGING FLOW CYTOMETRY



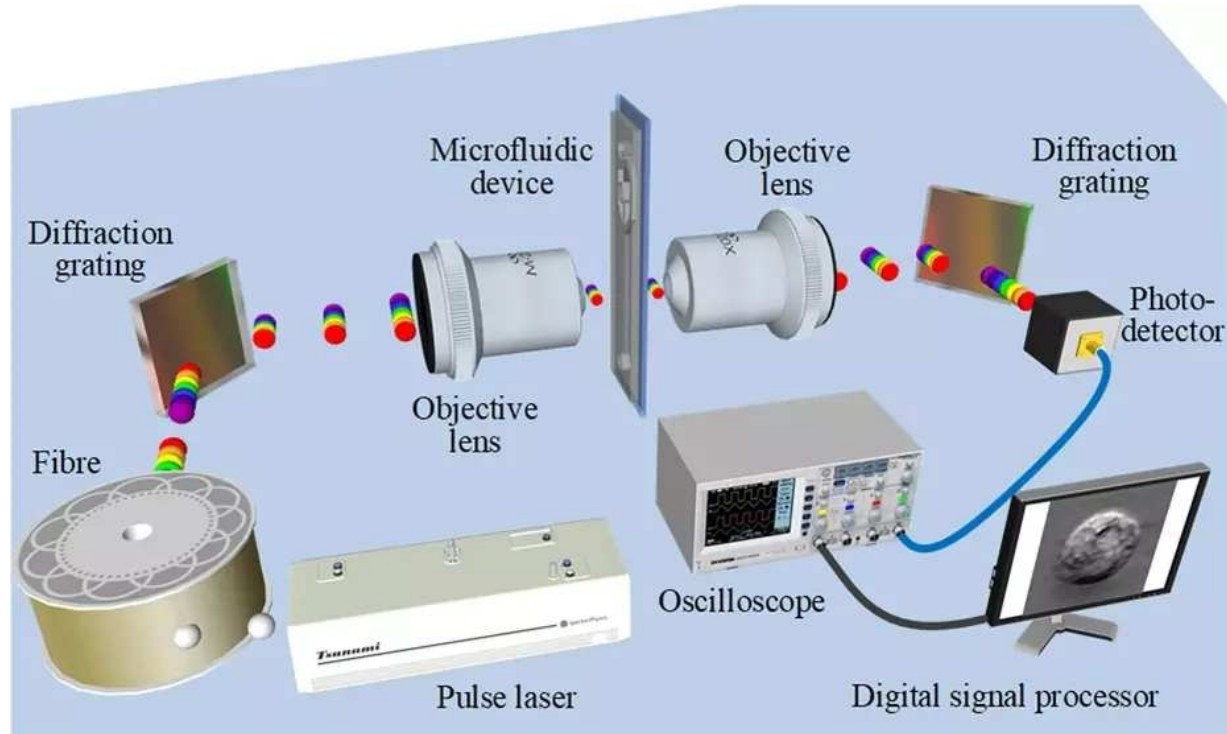
# LABEL-FREE IMAGING FLOW CYTOMETRY



Main bottlenecks:

- **computational cost** of classification
- camera frame rate (up to ~1000 particles/s)
  - ➔ but several holograms could be acquired in parallel

# HIGH THROUGHPUT IMAGING WITH OPTOFLUIDIC TIME-STRETCH MICROSCOPY

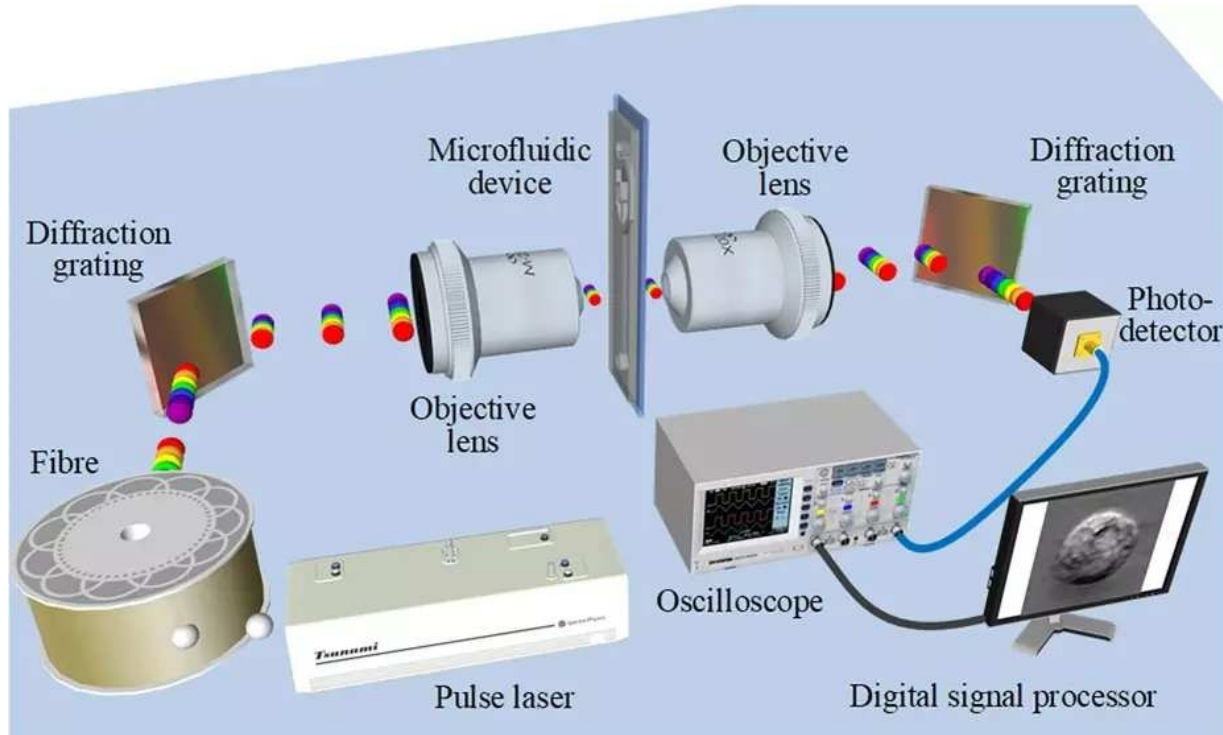


Hirofumi Kobayashi, et al. "Label-free detection of cellular drug responses by high-throughput bright-field imaging and machine learning". *Scientific reports*, 2017

License: Creative Commons Attribution: Attribution 4.0 International. <https://creativecommons.org/licenses/by/4.0/>. Accessed: 2021-04-30



# HIGH THROUGHPUT IMAGING WITH OPTOFLUIDIC TIME-STRETCH MICROSCOPY



→ Very high-throughput: up to 100,000 cells/s

But...

- Relatively expensive and complicated
- ~1Tbit/s of continuous measurement data!
  - online operation is desirable!
  - necessary for cell sorting
  - **need for computationally cheap analysis**

Hirofumi Kobayashi, et al. "Label-free detection of cellular drug responses by high-throughput bright-field imaging and machine learning". *Scientific reports*, 2017

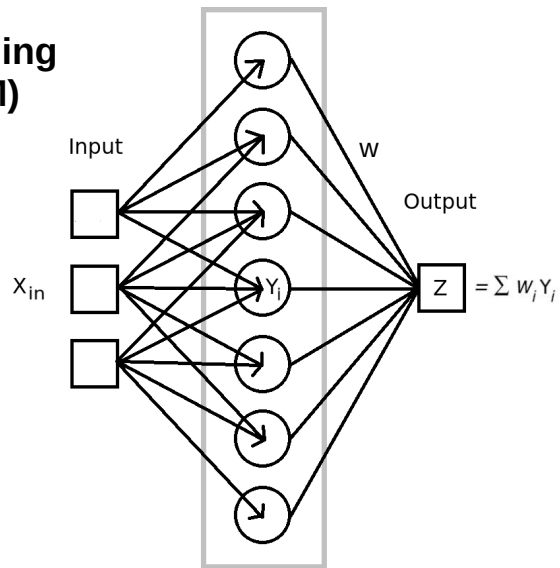
License: Creative Commons Attribution: Attribution 4.0 International. <https://creativecommons.org/licenses/by/4.0/>. Accessed: 2021-04-30



# A SHORTCUT TO EXPLOIT HARDWARE 'COMPUTATION'

nonlinear random transformation

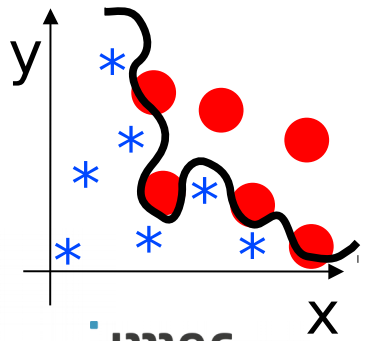
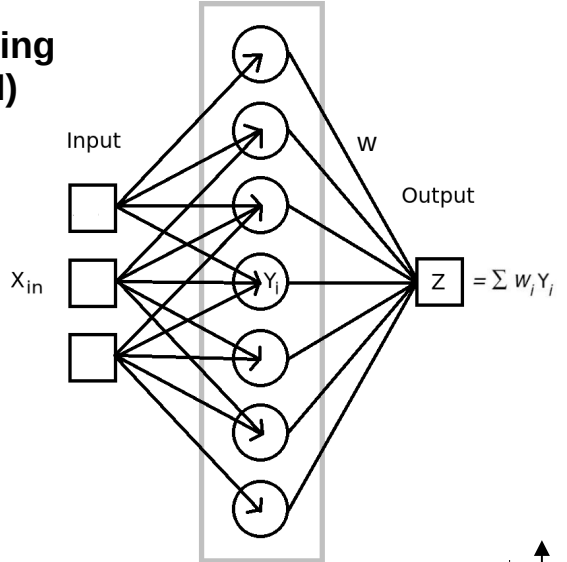
**Extreme learning machine (ELM)**



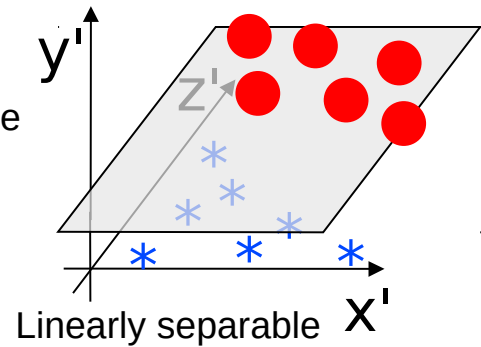
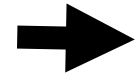
# HARDWARE-BASED RANDOM DIMENSIONALITY EXPANSION

Extreme learning machine (ELM)

nonlinear random transformation



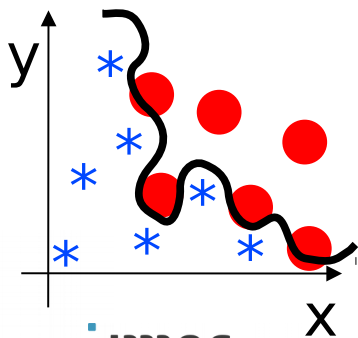
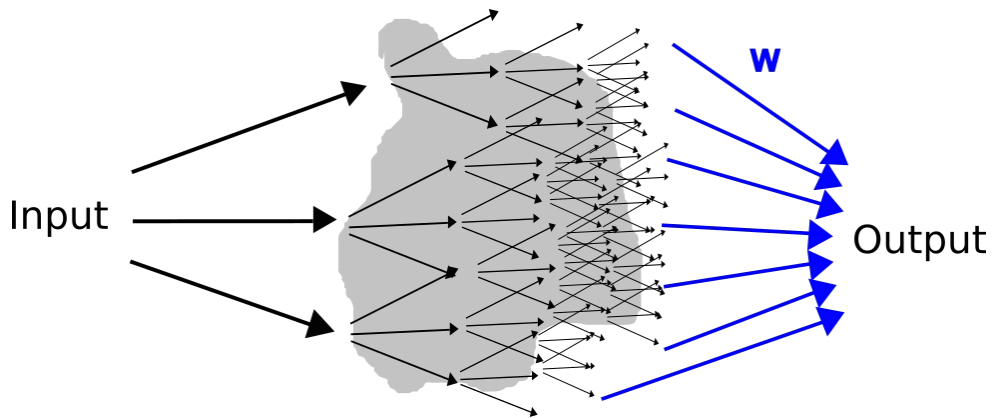
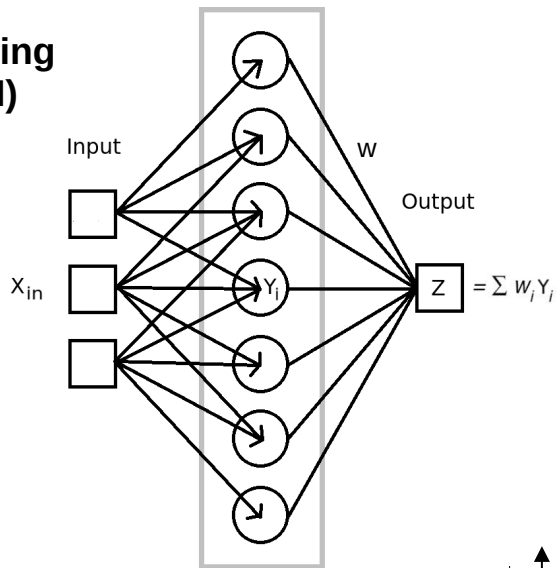
Map to a higher dimensional space



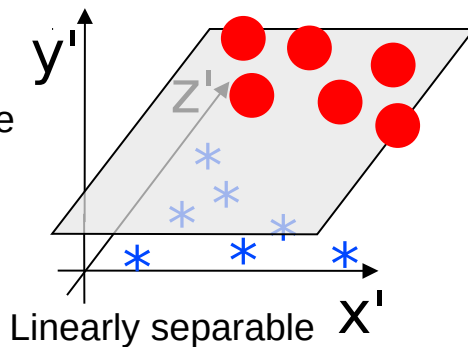
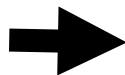
# HARDWARE-BASED RANDOM DIMENSIONALITY EXPANSION

## Extreme learning machine (ELM)

nonlinear random transformation



Map to a higher dimensional space



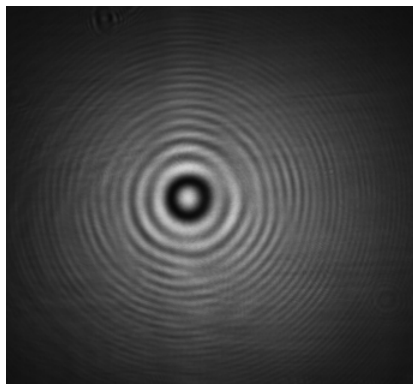
Suitable for **hardware implementations**

**Photonics:** high-speed, efficient parallel processing

# WHITE BLOOD CELL HOLOGRAM CLASSIFICATION

# REAL CELL HOLOGRAMS

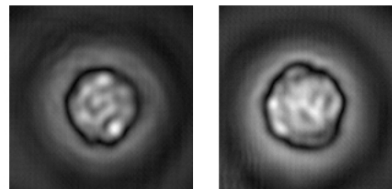
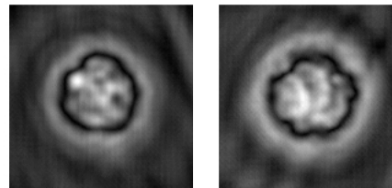
Raw hologram



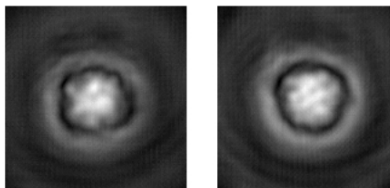
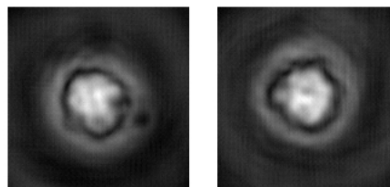
Reconstruction



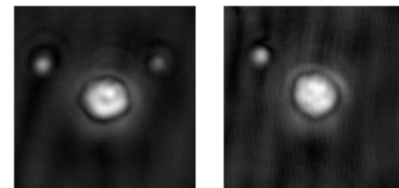
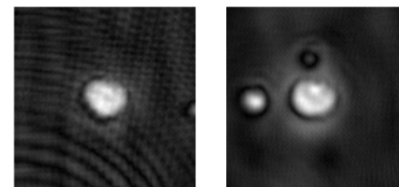
Granulocytes



Monocytes



T-lymphocytes



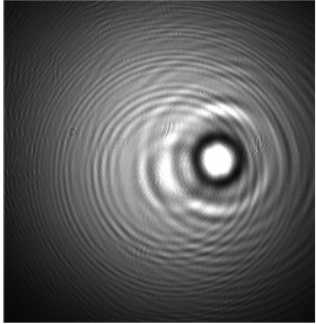
WBC holograms from Imec collaborators:

- 20,797 monocyte
- 3,753 T cell
- 32,514 granulocyte

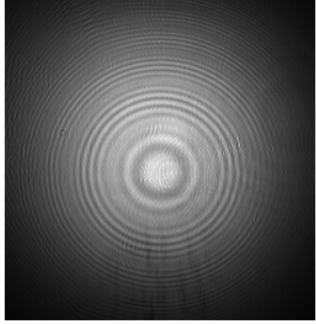
**Goal:** fast classification

# ADDRESSING HOLOGRAM VARIABILITY (NOISE)

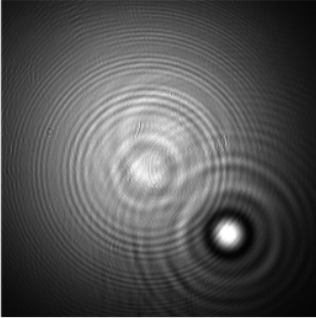
Single cell hologram



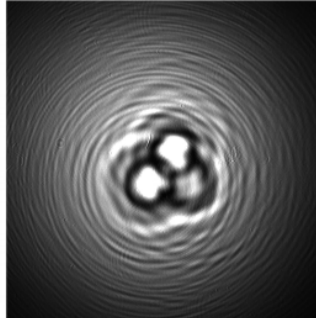
Background



Uncentered cell and reflection

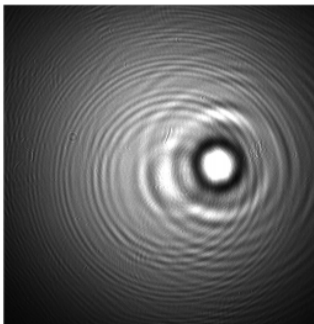


Two attached cells

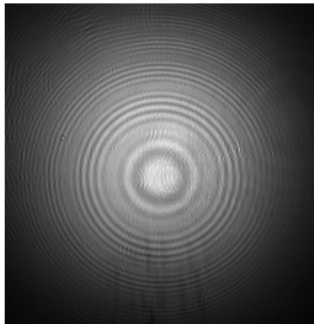


# ADDRESSING HOLOGRAM VARIABILITY (NOISE)

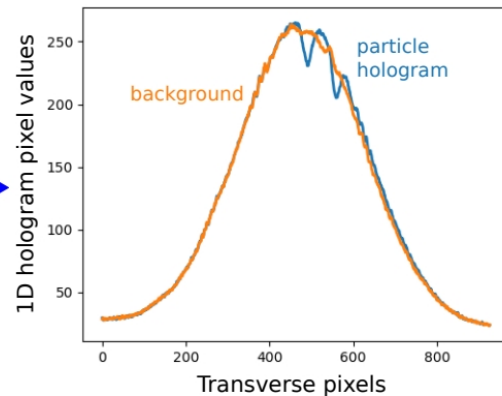
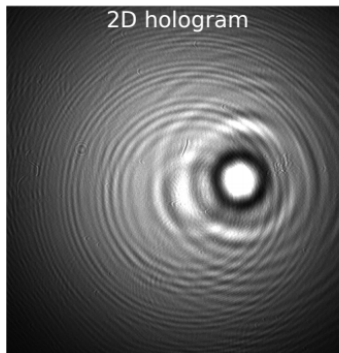
Single cell hologram



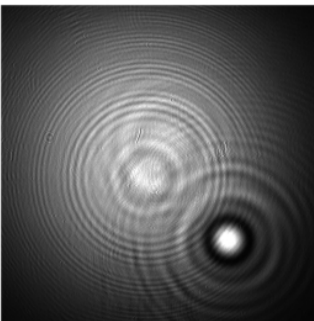
Background



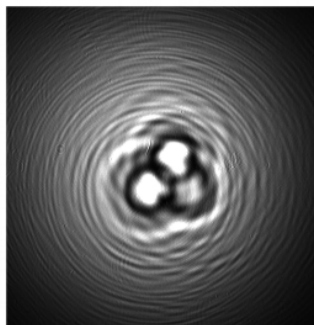
2D hologram



Uncentered cell and reflection

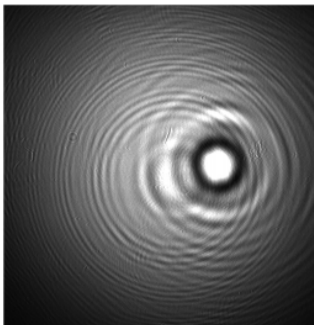


Two attached cells

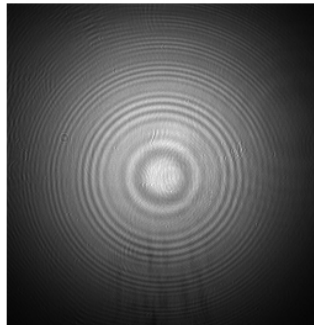


# ADDRESSING HOLOGRAM VARIABILITY (NOISE)

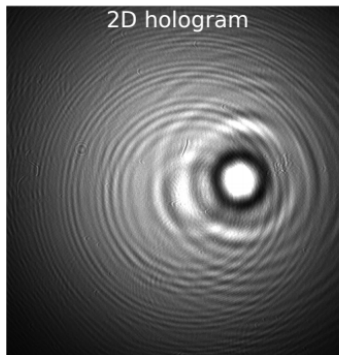
Single cell hologram



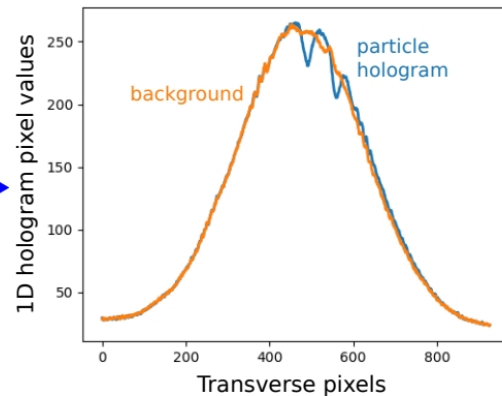
Background



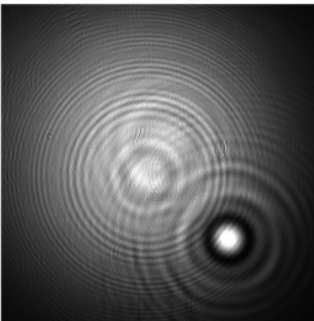
2D hologram



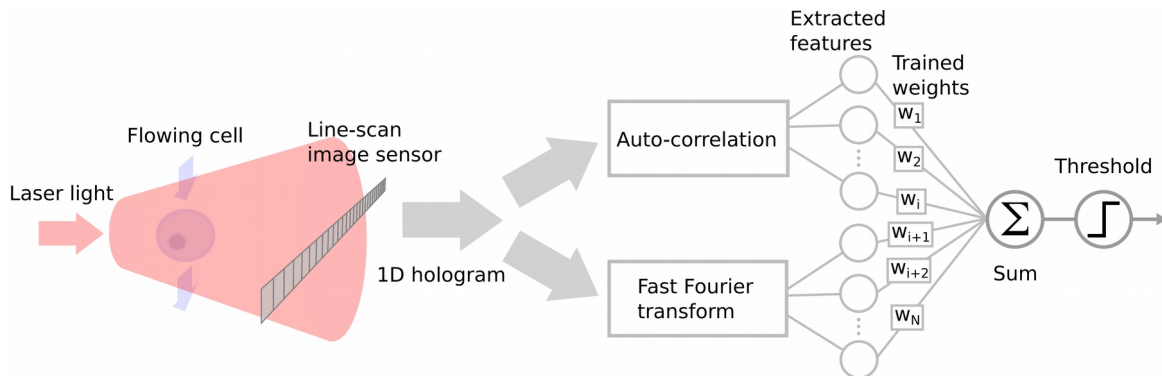
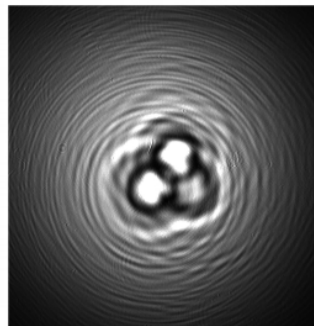
Integration



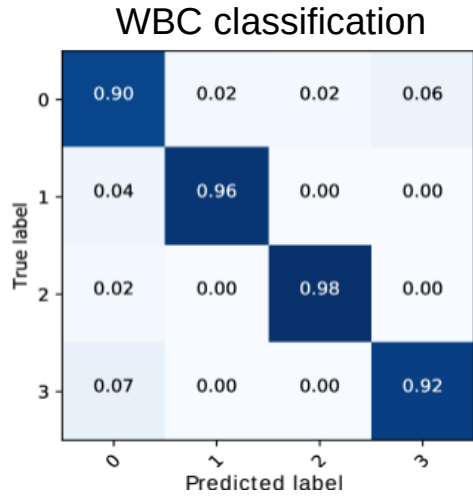
Uncentered cell and reflection



Two attached cells

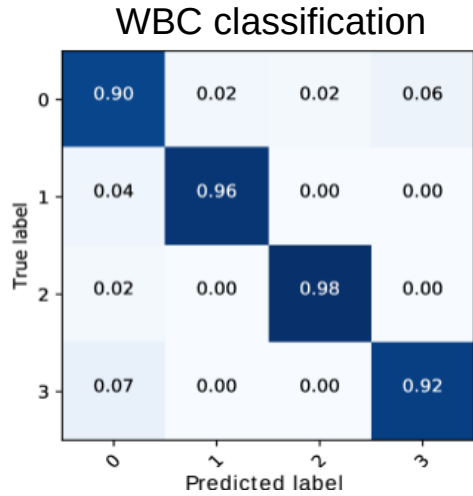


# SHORTCUT LEARNING!



High accuracy!

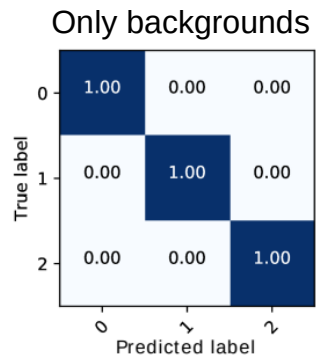
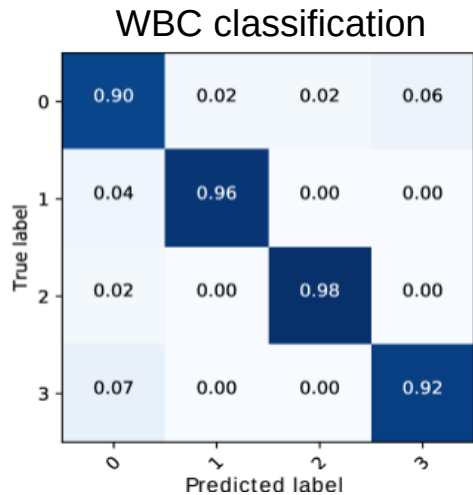
# SHORTCUT LEARNING!



High accuracy!

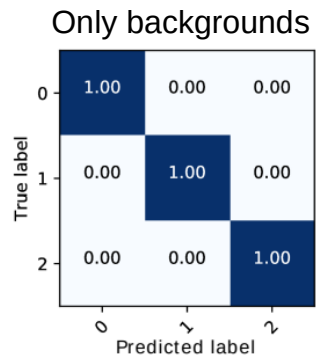
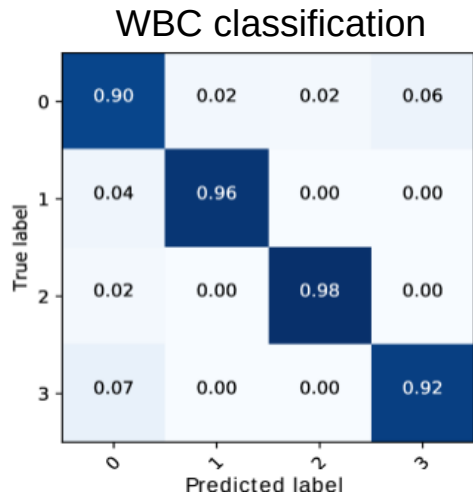


# SHORTCUT LEARNING!



High accuracy!

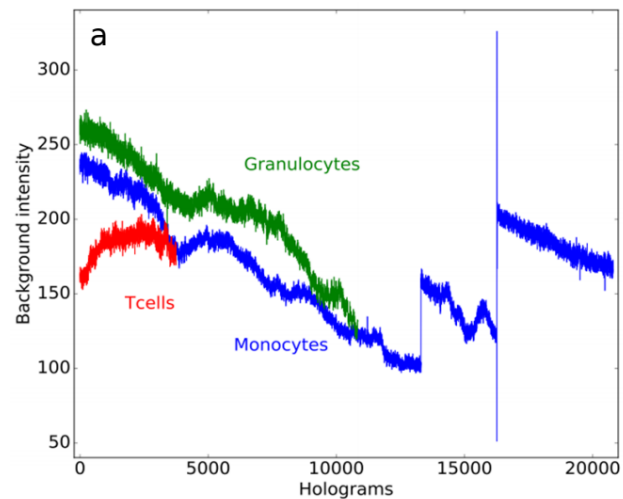
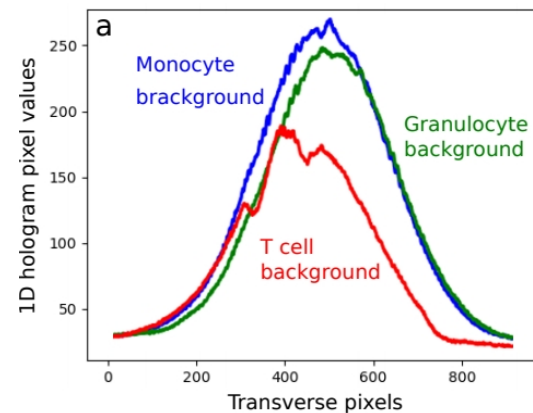
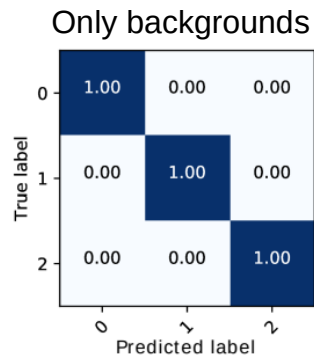
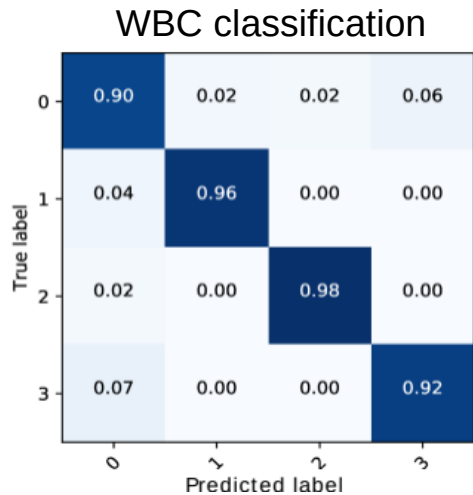
# SHORTCUT LEARNING!



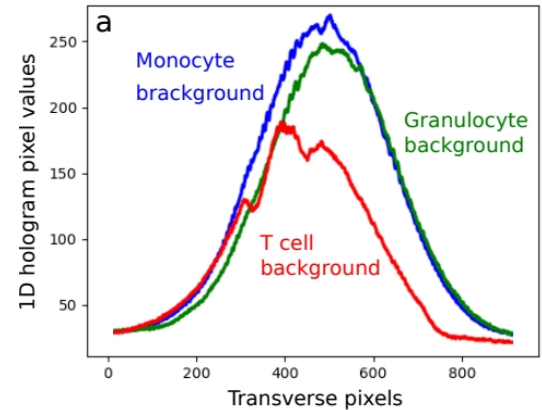
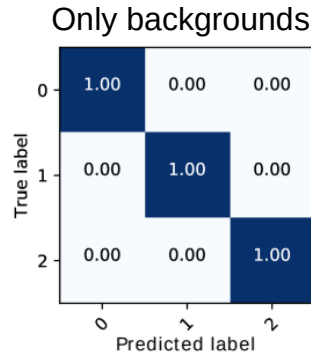
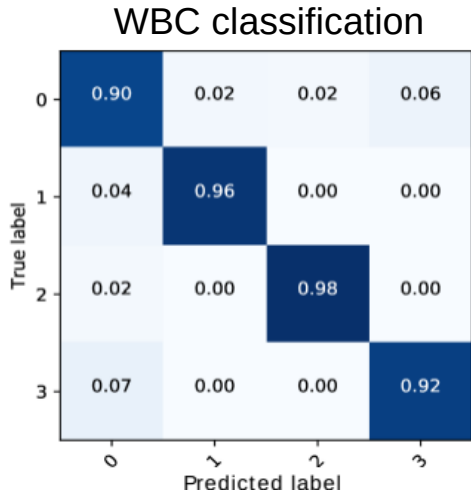
High accuracy!



# SHORTCUT LEARNING!



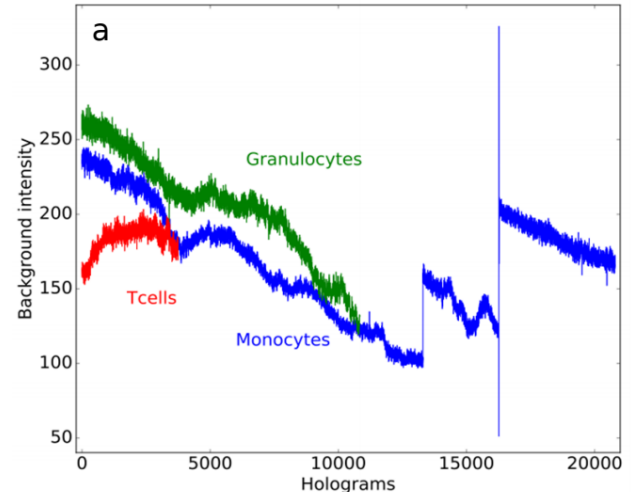
# SHORTCUT LEARNING!



**Shortcut learning** (*measurement bias*): often ignored or underestimated

Geirhos, R., et al. "Shortcut learning in deep neural networks." *Nat. Mach. Intell.*, 2020

- Cross-validation does not help
- Background subtraction is not sufficient



# TREATMENT OF MEASUREMENT BIAS

Measurement bias is a two-fold problem:

- 1) undermines learning
- 2) **test results are inflated**

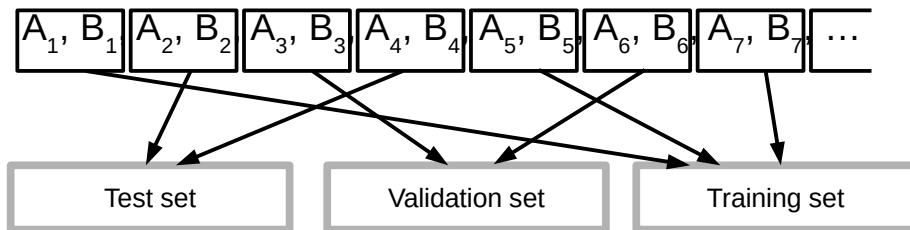
# TREATMENT OF MEASUREMENT BIAS

Measurement bias is a two-fold problem:

- 1) undermines learning
- 2) **test results are inflated**

**Intertwined class measurements** address both:

$A_1, B_1, A_2, B_2, A_3, B_3, A_4, B_4, A_5, B_5, A_6, B_6, A_7, B_7, \dots$



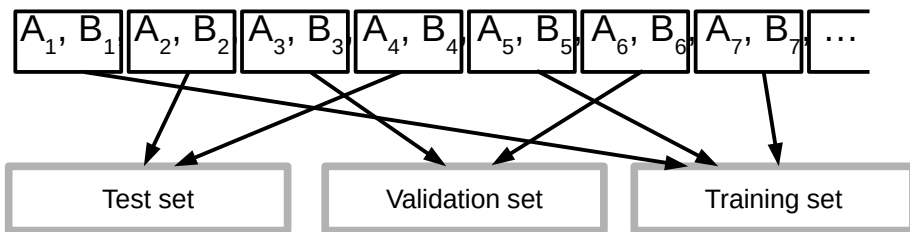
# TREATMENT OF MEASUREMENT BIAS

Measurement bias is a two-fold problem:

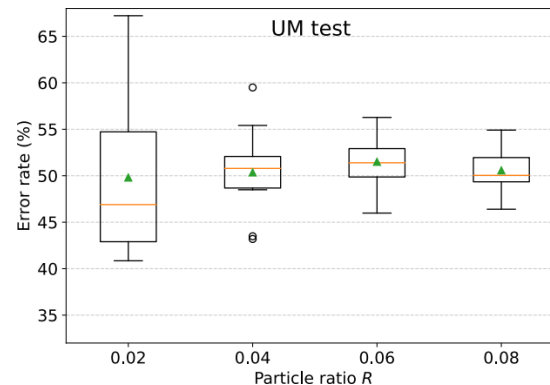
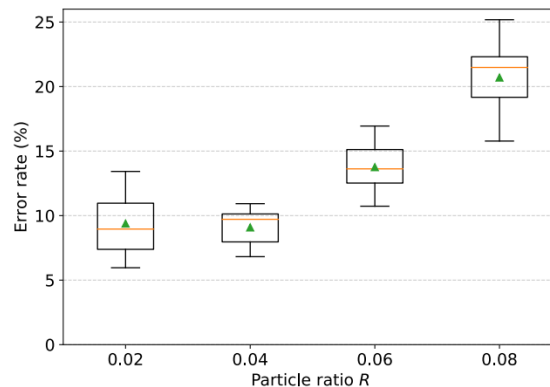
- 1) undermines learning
- 2) test results are inflated

**Intertwined class measurements** address both:

$A_1, B_1, A_2, B_2, A_3, B_3, A_4, B_4, A_5, B_5, A_6, B_6, A_7, B_7, \dots$

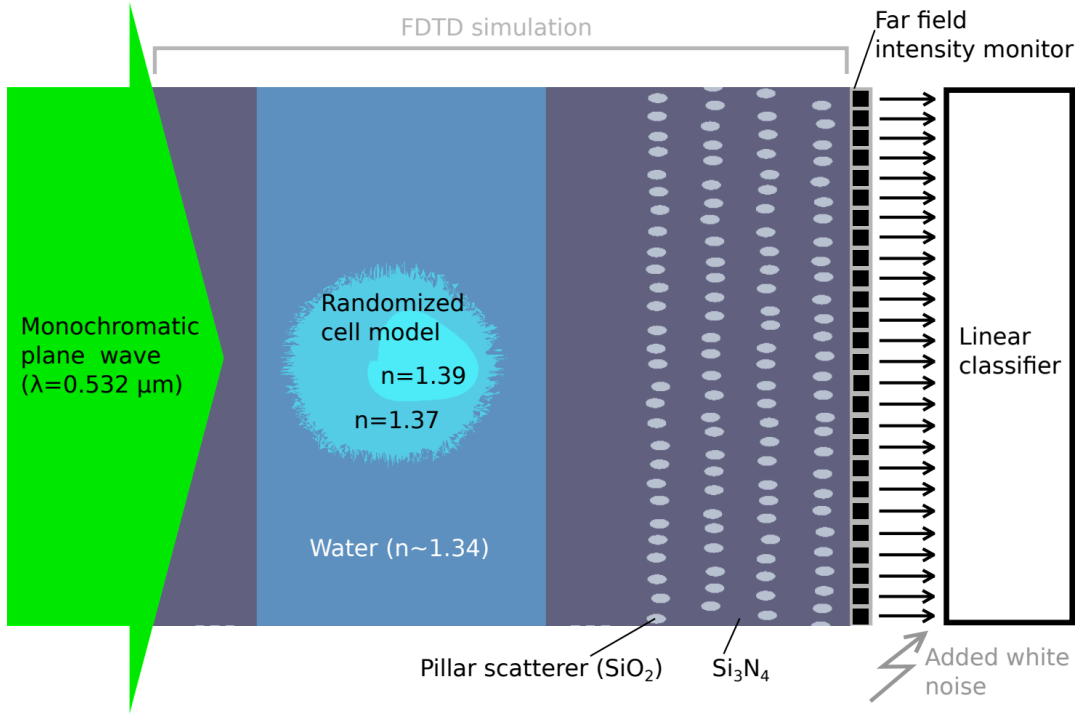


**Effectiveness demonstrated** in dedicated experiment with microspheres:



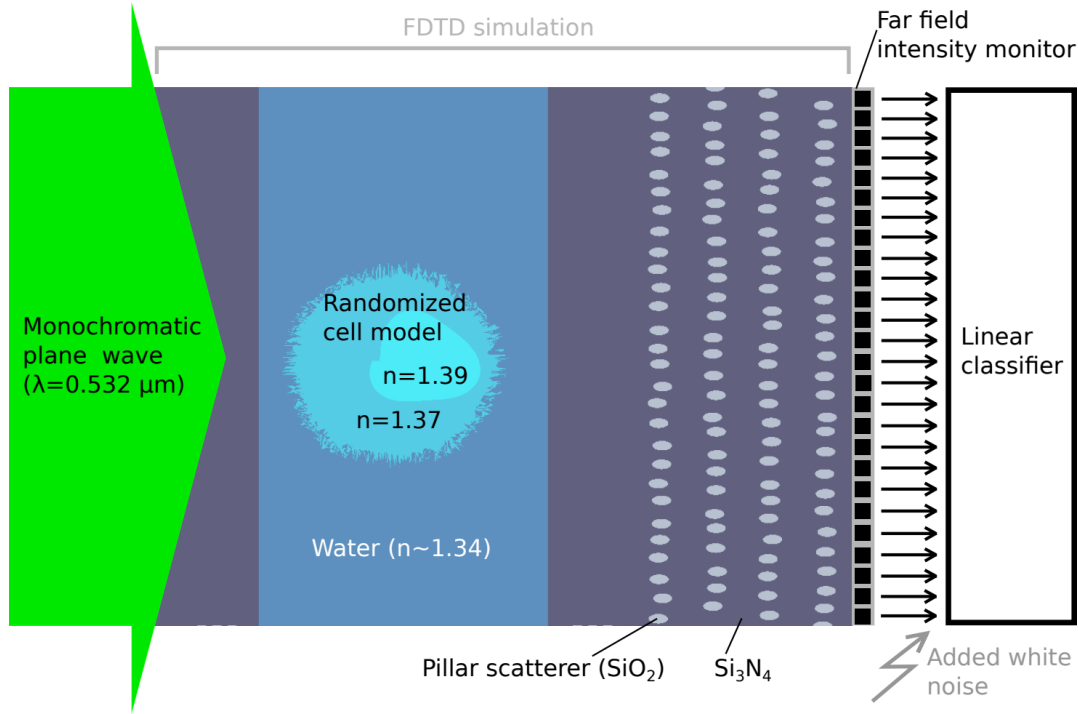
# DIMENSIONALITY EXPANSION WITH DIELECTRIC SCATTERERS

# RANDOMIZED SIMULATIONS OF CELL ILLUMINATION

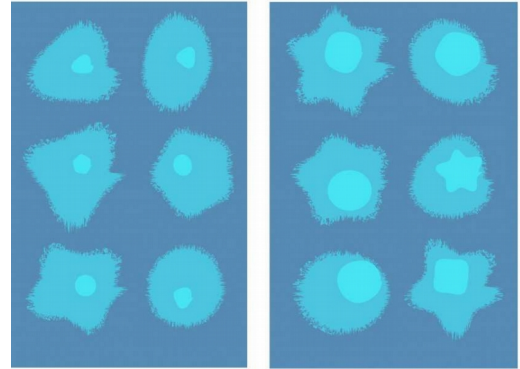


7200 FDTD simulations per scatterer configuration

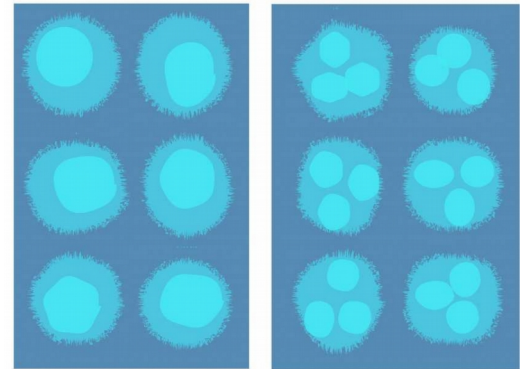
# RANDOMIZED SIMULATIONS OF CELL ILLUMINATION



Task 1: nucleus size

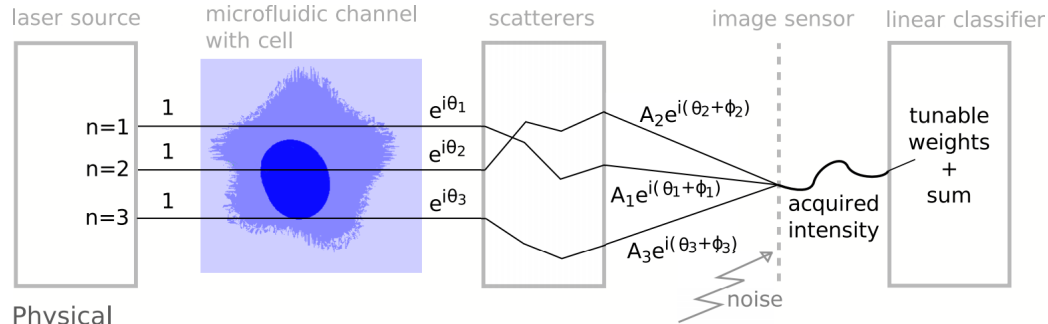


Task 2: nucleus shape



7200 FDTD simulations per scatterer configuration

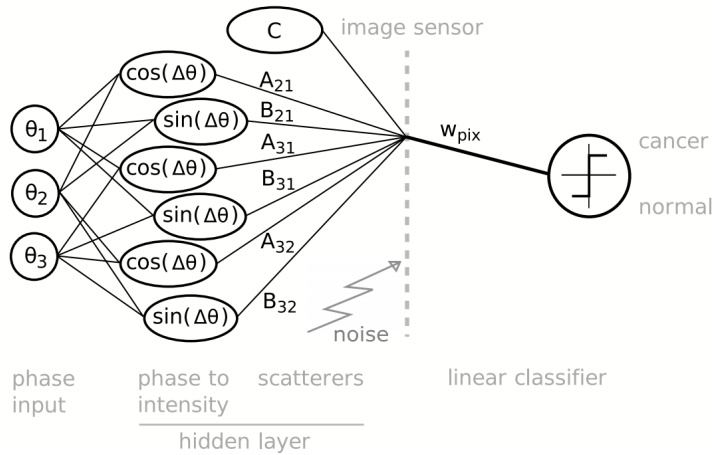
# NONLINEARITY AND ELM EQUIVALENCE



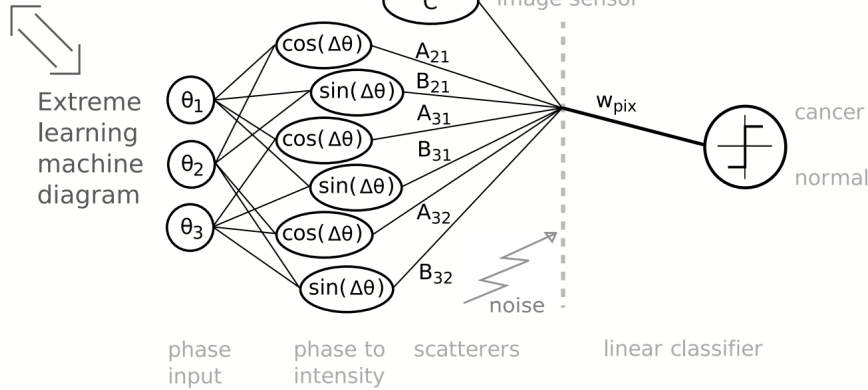
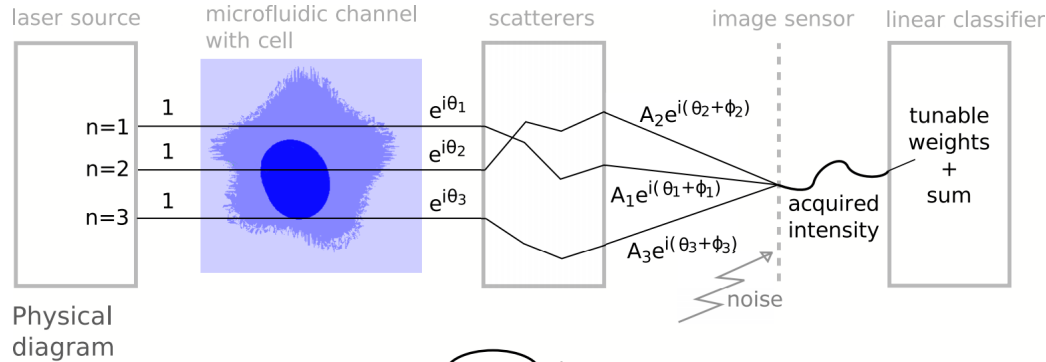
Physical diagram



Extreme learning machine diagram

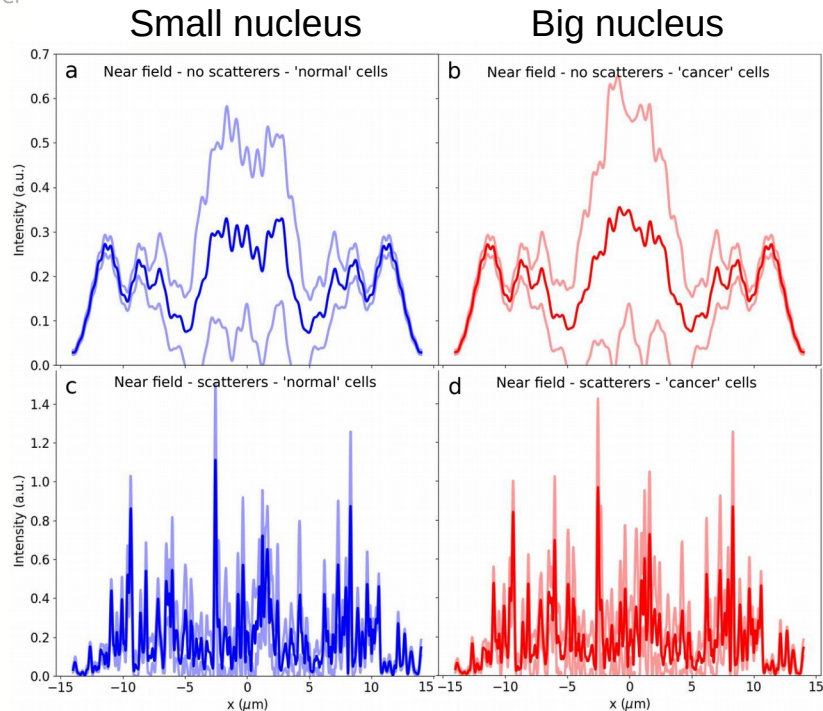
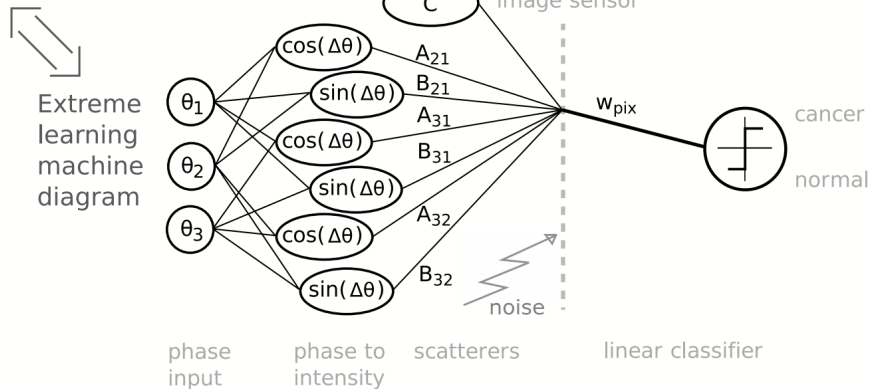
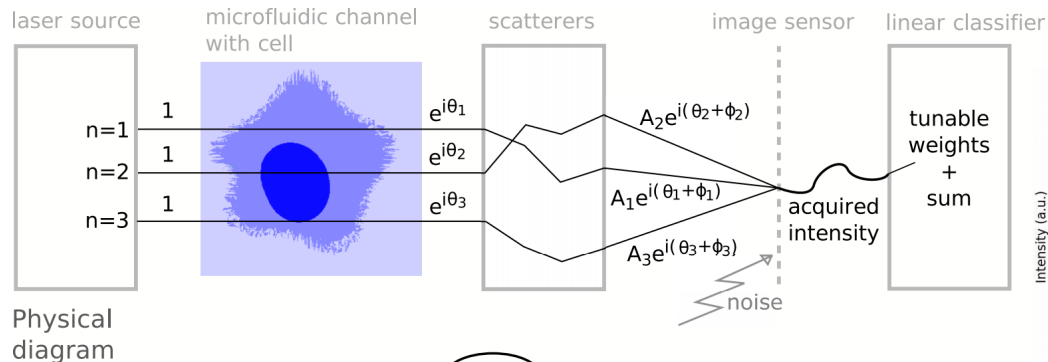


# NONLINEARITY AND ELM EQUIVALENCE



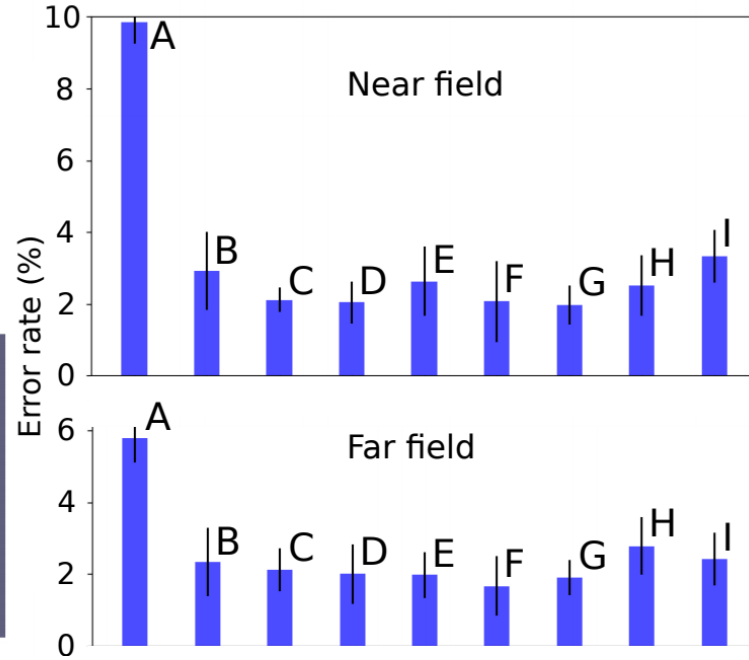
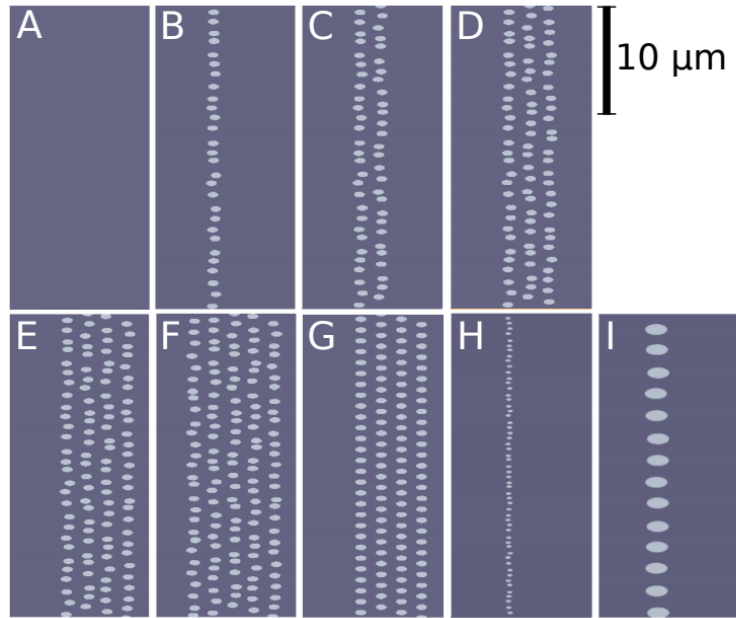
$$I \propto \left| \sum_n A_n e^{i(\theta_n + \phi_n)} \right|^2 = C + \sum_{m < n} [A_{nm} \cos(\theta_n - \theta_m) + B_{nm} \sin(\theta_n - \theta_m)]$$

# NONLINEARITY AND ELM EQUIVALENCE



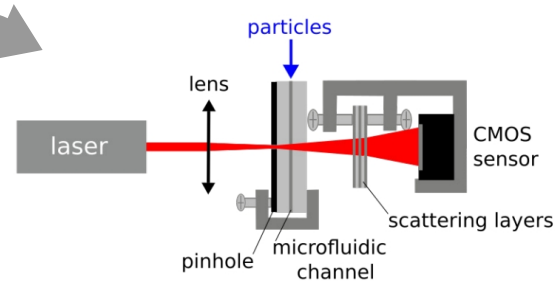
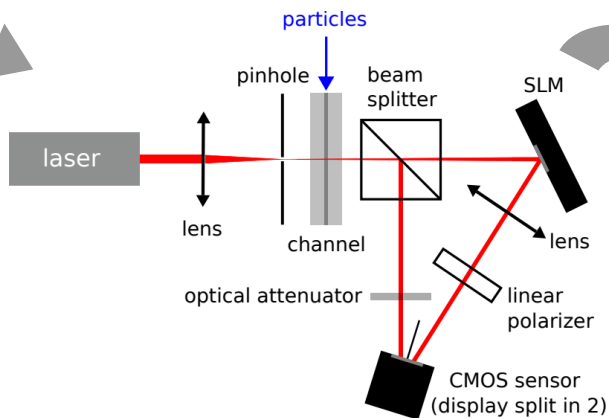
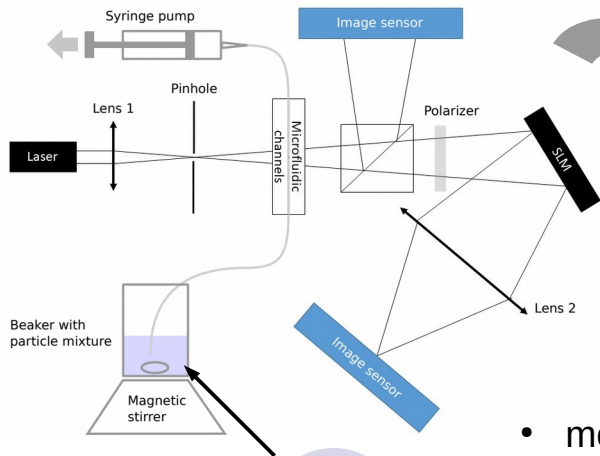
$$I \propto \left| \sum_n A_n e^{i(\theta_n + \phi_n)} \right|^2 = C + \sum_{m < n} [A_{nm} \cos(\theta_n - \theta_m) + B_{nm} \sin(\theta_n - \theta_m)]$$

# EXPLORATION OF SCATTERER CONFIGURATION

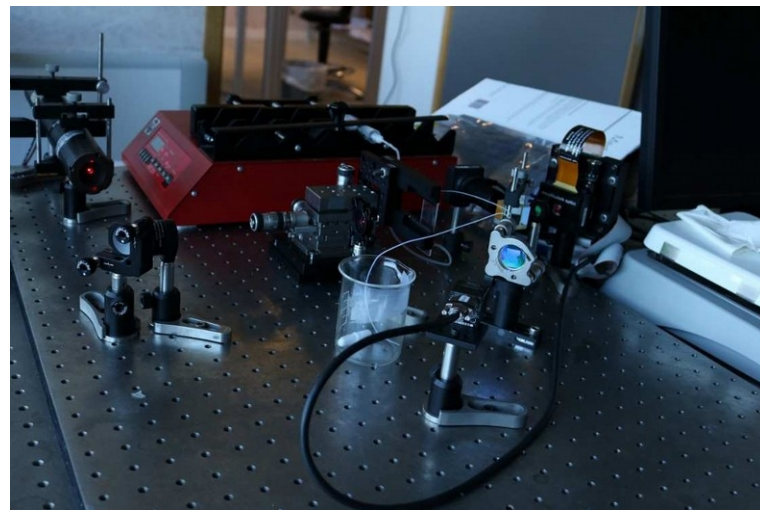


# DEVELOPMENT OF FLOW CYTOMETRY EXPERIMENT

# SETUP EVOLUTION



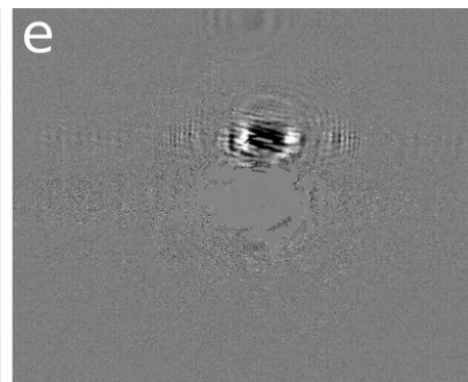
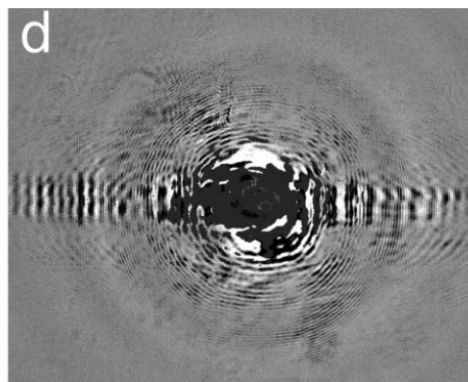
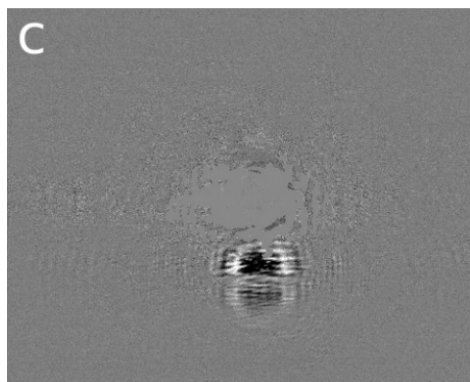
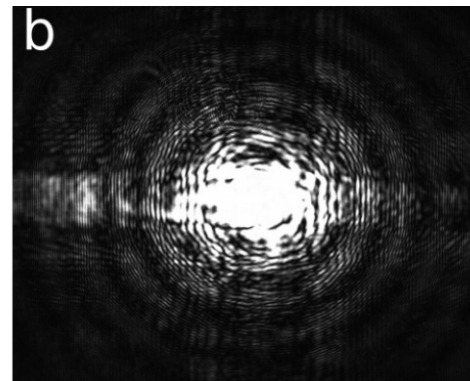
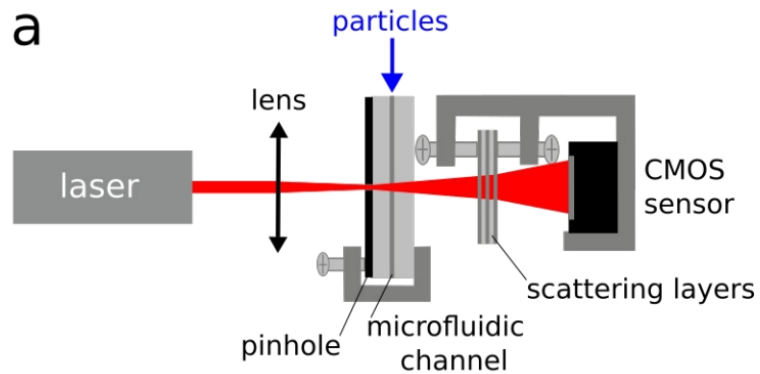
- measurement bias
- signal-to-background ratio
- bubbles or dirt
- vibrations
- background detection and subtraction
- SLM flicker
- feature selection
- exploration and selection of scattering media
- few-samples estimation
- motion blur



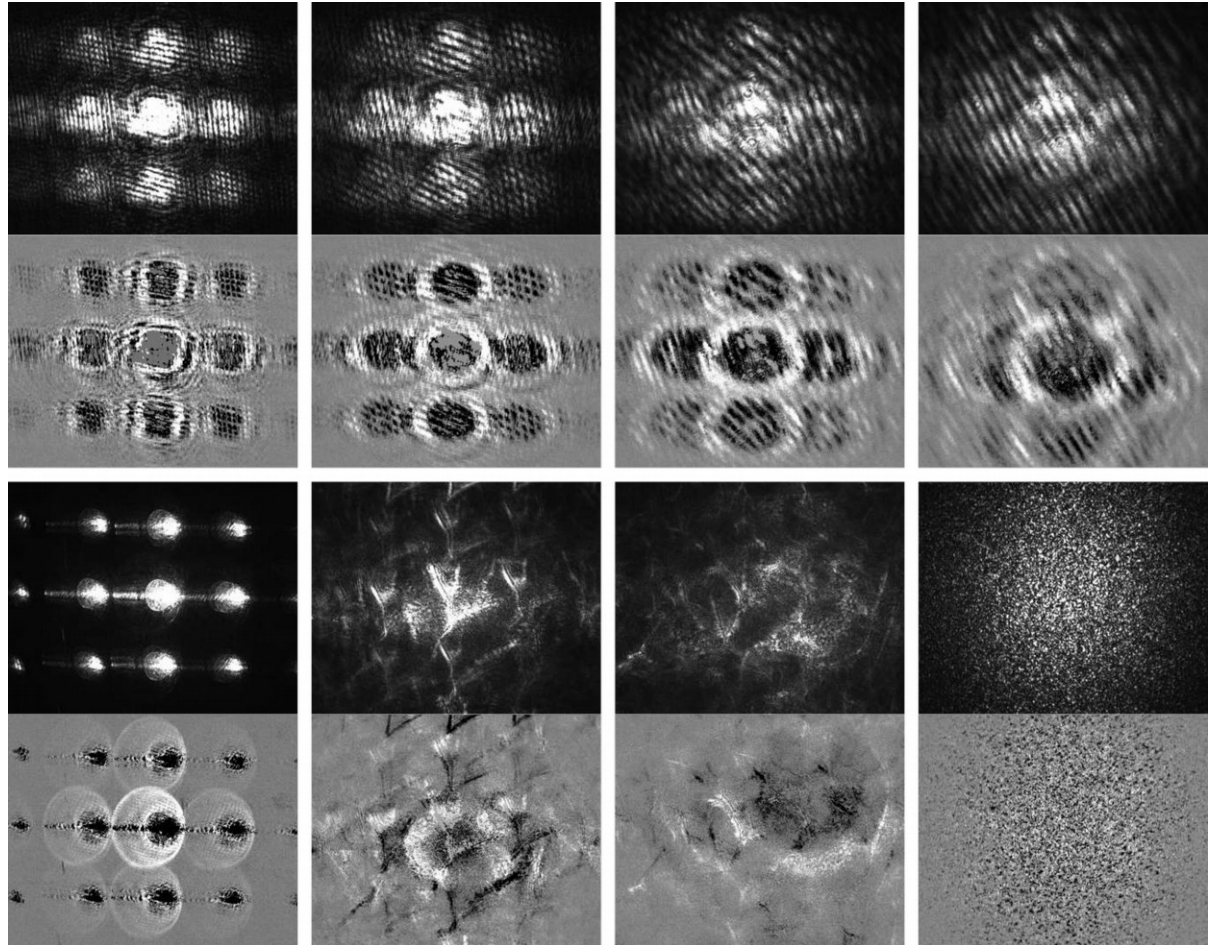
# HIGH SNR IN ACQUIRED PATTERNS

15 $\mu\text{m}$

18 $\mu\text{m}$



# EXPLORATION OF SCATTERING LAYERS

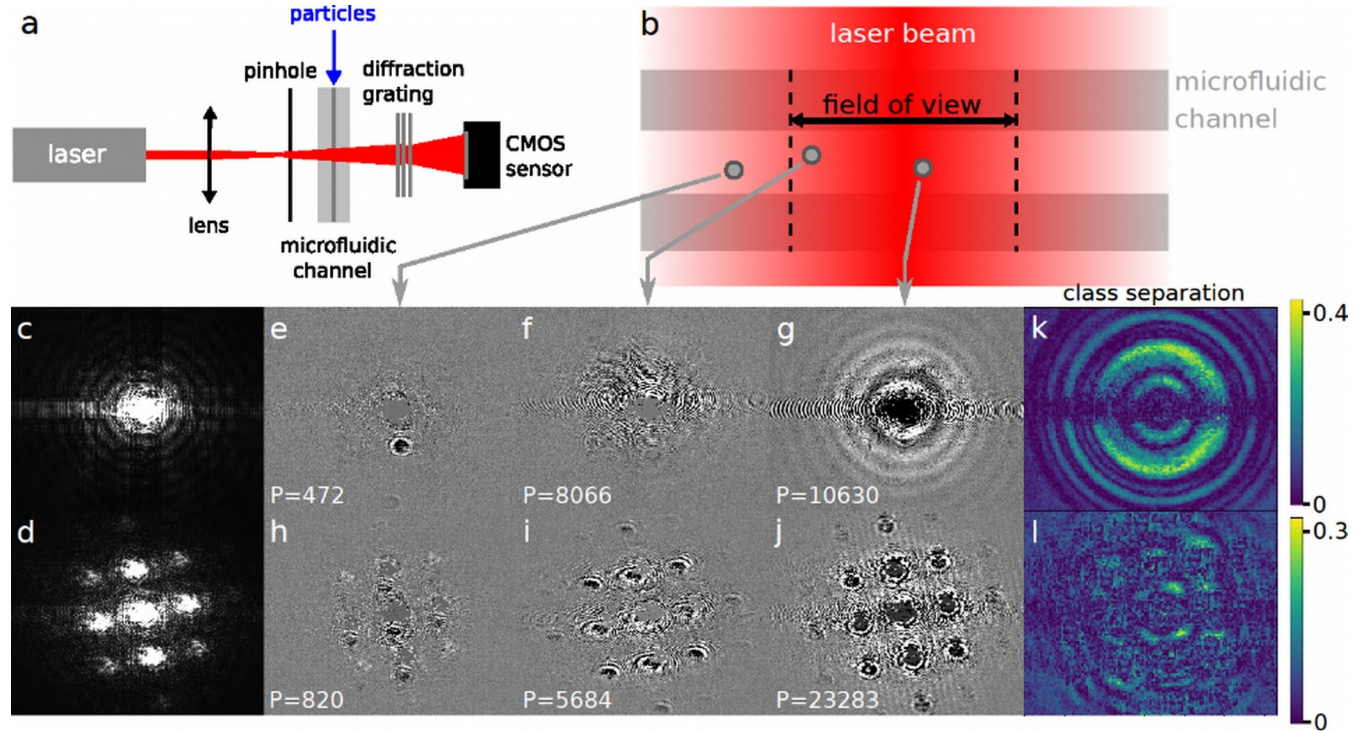


More than 40 configurations tested!

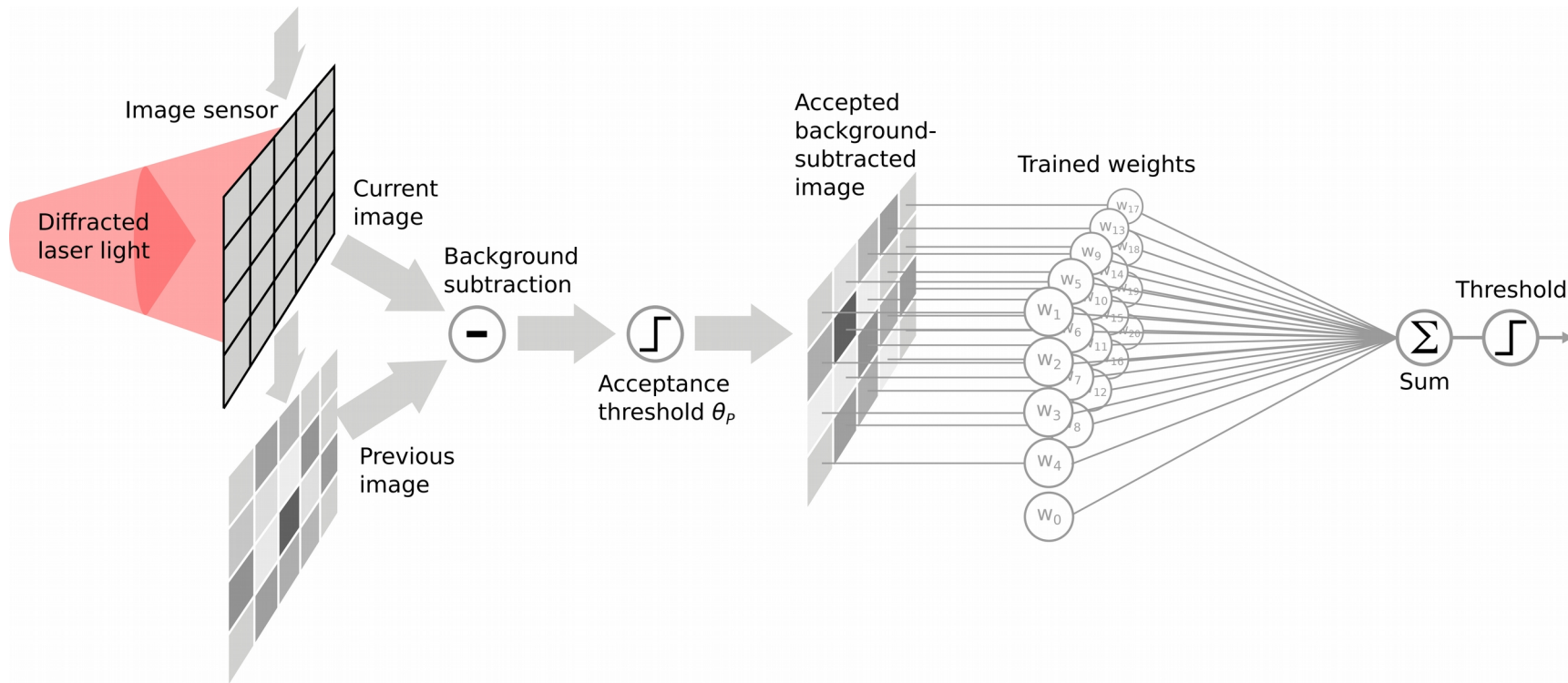
# FINAL EXPERIMENT RESULTS

# FINAL EXPERIMENT

- No focusing
- Large field of view
- Cheap and simple components



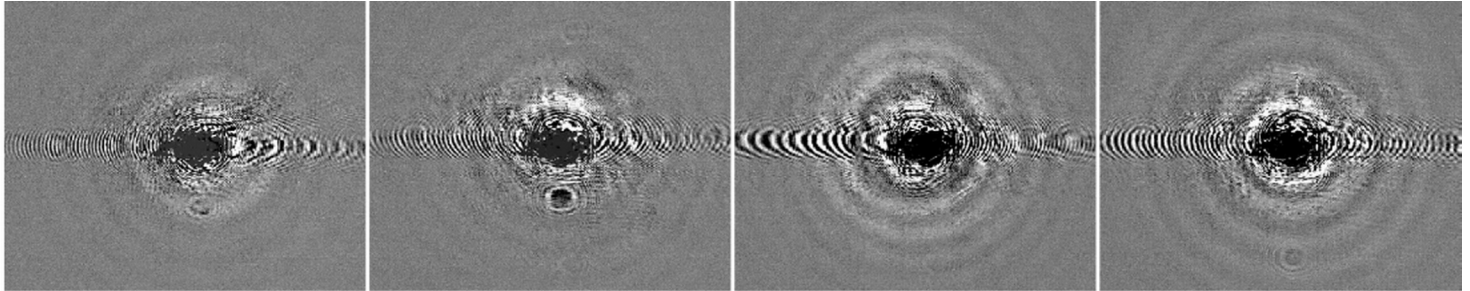
# A SIMPLE, FAST AND VERSATILE CLASSIFIER



# PATTERNS FROM DIFFERENT CLASSES

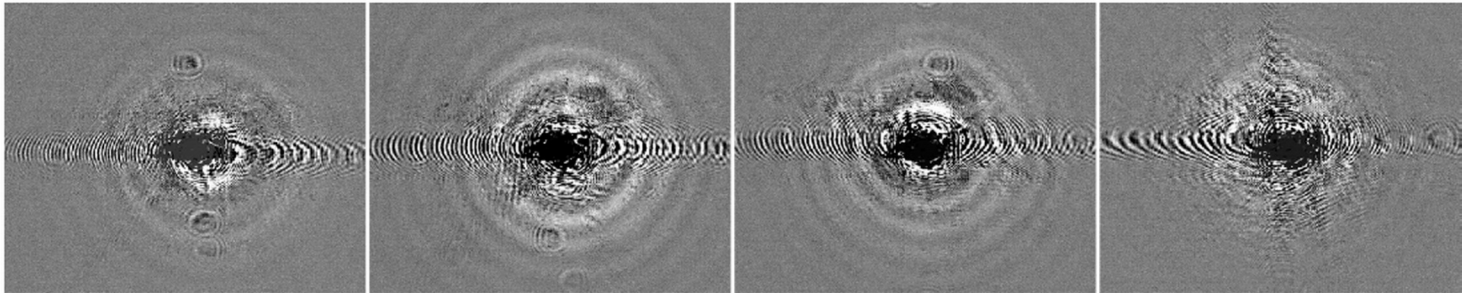
15 $\mu$ m

Class A

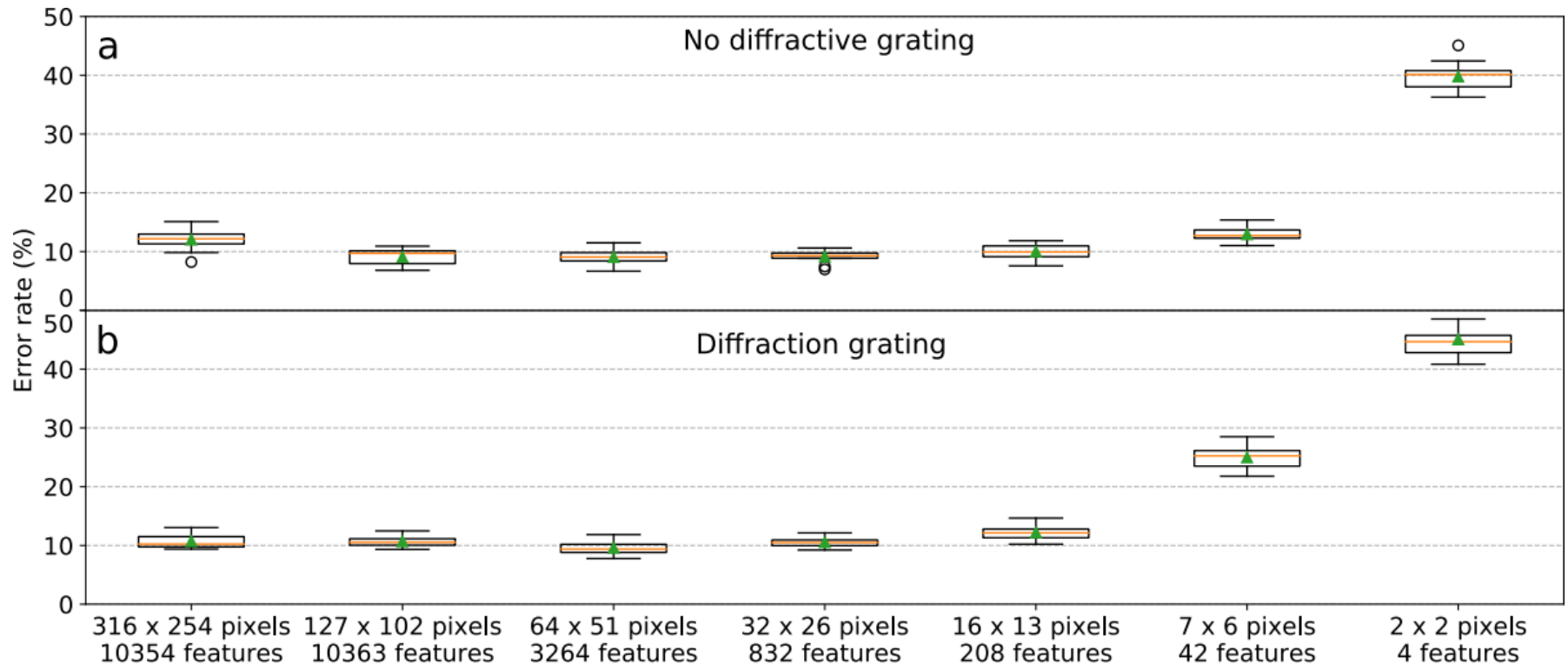


18 $\mu$ m

Class B



# ERROR V.S. IMAGE RESOLUTION



# COMPARISON WITH OTHER WORKS

	Classification task	Classifier	Image resolution	Imaging method	Image FoV	Classification performance	Accelerator	execution time / particle	Meas. bias control
[1]	Beads with diameters of 7, 10 and 15 $\mu\text{m}$	CNN	$21 \times 21$	Microscope	Centered and cropped	93.3% mAP	GPU	< 1 ms	Unreported
[2]	3 white blood cell (WBC) types	Rand. forest on extracted features	$31 \times 31$	Lens-free - raw hologram	Unreported	96.8% accuracy	GPU	0.2 ms	Unreported
[3]	1 WBC type and an epithelial cancer cell	Deep CNN	Unreported	Time-stretch microscope	25 $\mu\text{m}$ along channel	95.74% accuracy	GPU	3.6 ms	Unreported
	Beads with diameters of 15.2 and 18.6 $\mu\text{m}$ (our work)	Linear (log. regression)	$32 \times 26$	Lens-free - raw hologram	$\sim 300 \mu\text{m}$ along channel	> 90% accuracy	None	0.013 ms	Yes

Potentially close to  $\sim 100,000$  cell/s

- [1] Heo, Young Jin, *et al.* "Real-time image processing for microscopy-based label-free imaging flow cytometry in a microfluidic chip". *Scientific Reports*, 2017.
- [2] Cornelis, B., *et al.* "Fast and robust Fourier domain-based classification for on-chip lens-free flow cytometry." *Optics Express*, 2018.
- [3] Li, Yueqin, *et al.* "Deep cytometry: deep learning with real-time inference in cell sorting and flow cytometry." *Scientific Reports*, 2019.

# CONCLUSIONS

- A simple **linear classifier** can be applied to particle holograms to provide **ultra-fast classification** in label-free flow cytometry
- On **condition** that:
  - the **extreme learning machine** paradigm is considered
  - the **shortcut learning** due to varying measurement conditions is properly treated (we demonstrated a suitable methodology)
- The demonstrated approach is **simple** to employ, **versatile** and require few **cheap** components

# CONCLUSIONS

- A simple **linear classifier** can be applied to particle holograms to provide **ultra-fast classification** in label-free flow cytometry
- On **condition** that:
  - the **extreme learning machine** paradigm is considered
  - the **shortcut learning** due to varying measurement conditions is properly treated (we demonstrated a suitable methodology)
- The demonstrated approach is **simple** to employ, **versatile** and require few **cheap** components

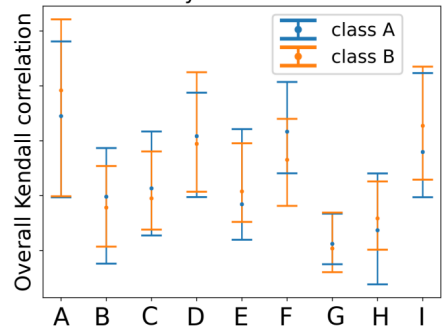
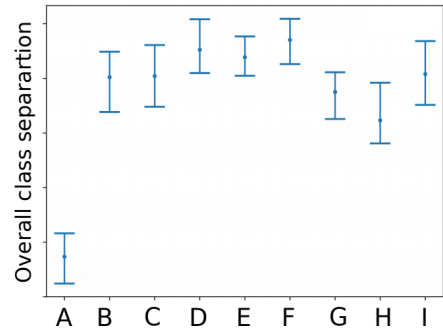
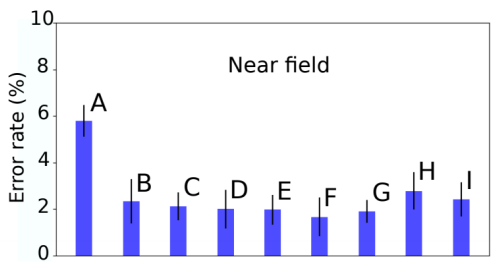
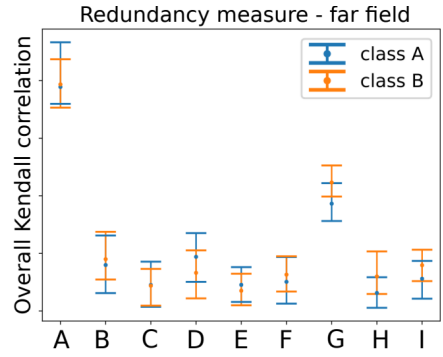
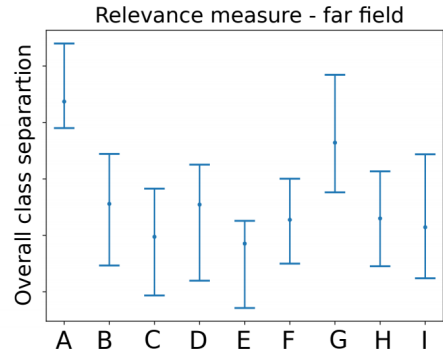
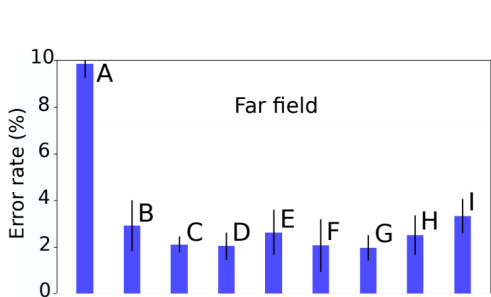
# FUTURE PERSPECTIVES

- High-throughput with high-speed **event-based camera** (Muhammed Gouda in Neoteric project)
- Apply our method to **cell classification** (e.g. WBC)
- Apply method to **existent high-throughput imaging systems** (e.g. time-stretch microscopy) to enable online operations
- Can scattering layers improve classification in **single-pixel configuration**?

# INTERPRETATION OF “DIMENSIONALITY EXPANSION”

Dimensionality expansion → Possible meanings: 1) more features per samples  
 2) more uncorrelated features } redundancy  
 3) **more relevant and uncorrelated features** } noise

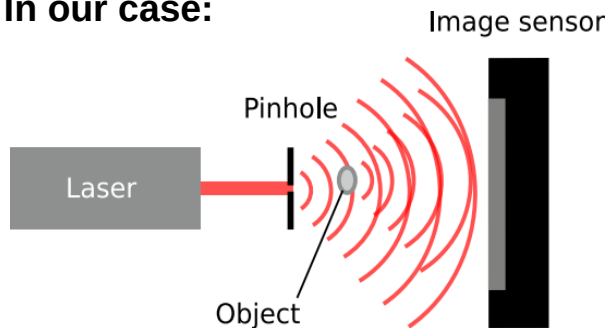
↓  
 Enhanced linear separability



# A SHORTCUT LEARNING EXAMPLE

Task to learn:  
distinguish seabirds from crows in a picture

In our case:



$$h_i - h_{i-1} = \delta h_i^{\text{bkgr}} + \mathcal{N}(h_i^{\text{bkgr}}, C_i)$$

Nonlinear interaction between cell information and background  
→ **need to act on measurements!**

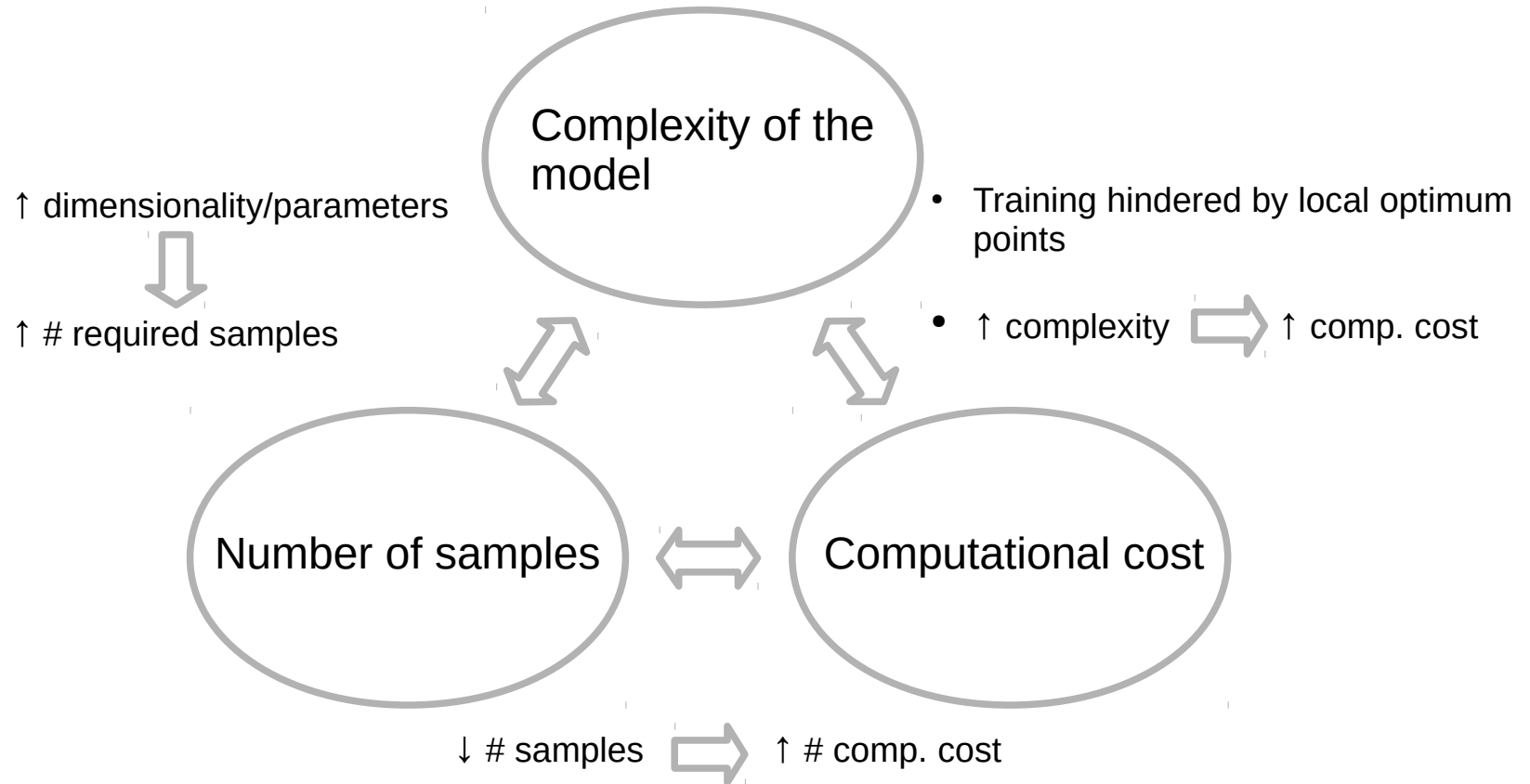
Seabird examples



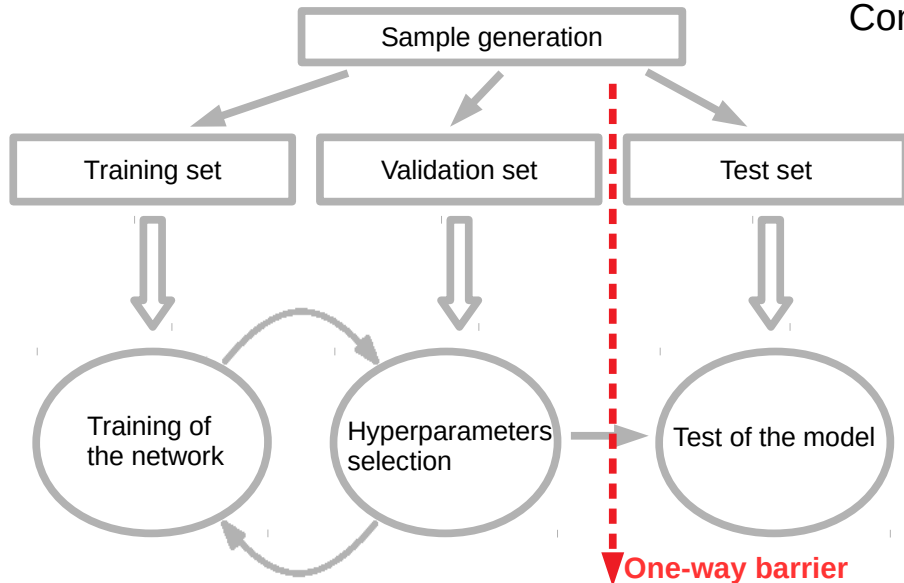
Crow examples



# TRADE-OFFS



# TREATMENT OF MEASUREMENT BIAS

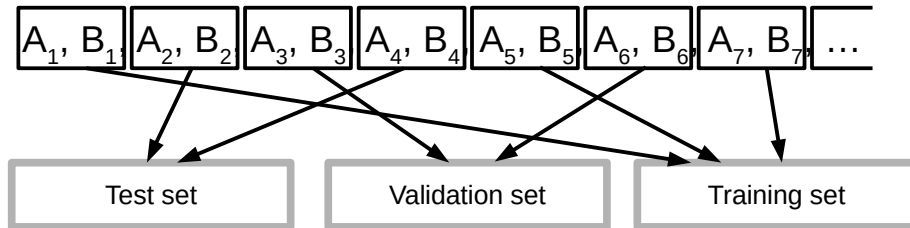


Conventional validation methods do not solve the problem

- Measurement bias is an **elusive, two-fold** problem:
- 1) sidetracks the training algorithm → undermines learning
  - 2) performance evaluation is also biased → test accuracy is inflated

**Intertwined class measurements** address both:

$A_1, B_1, A_2, B_2, A_3, B_3, A_4, B_4, A_5, B_5, A_6, B_6, A_7, B_7, \dots$

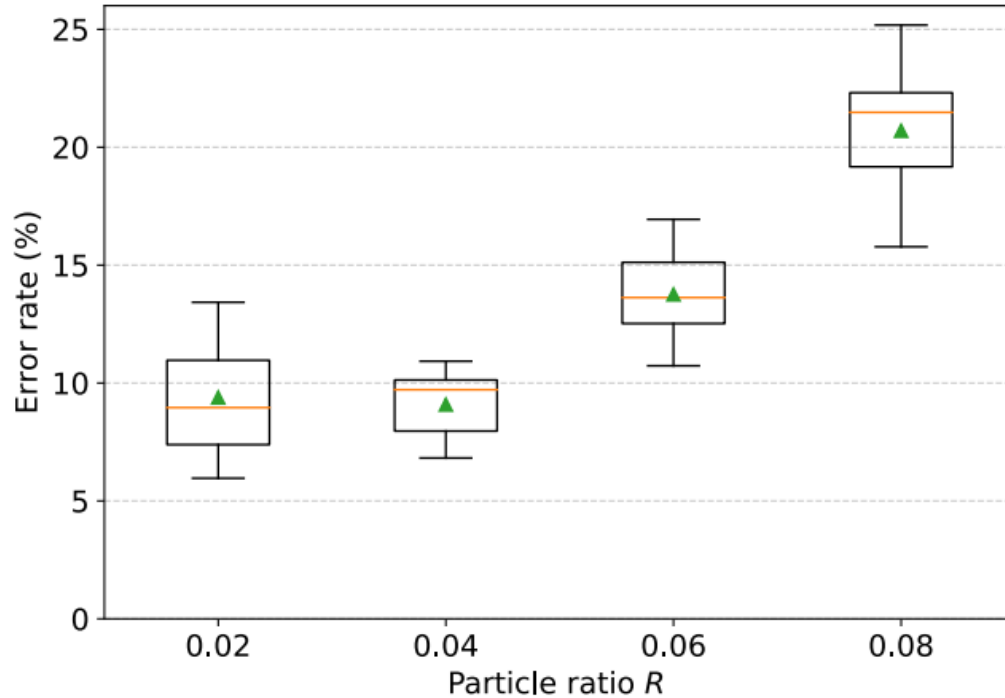


In Chapter 5:

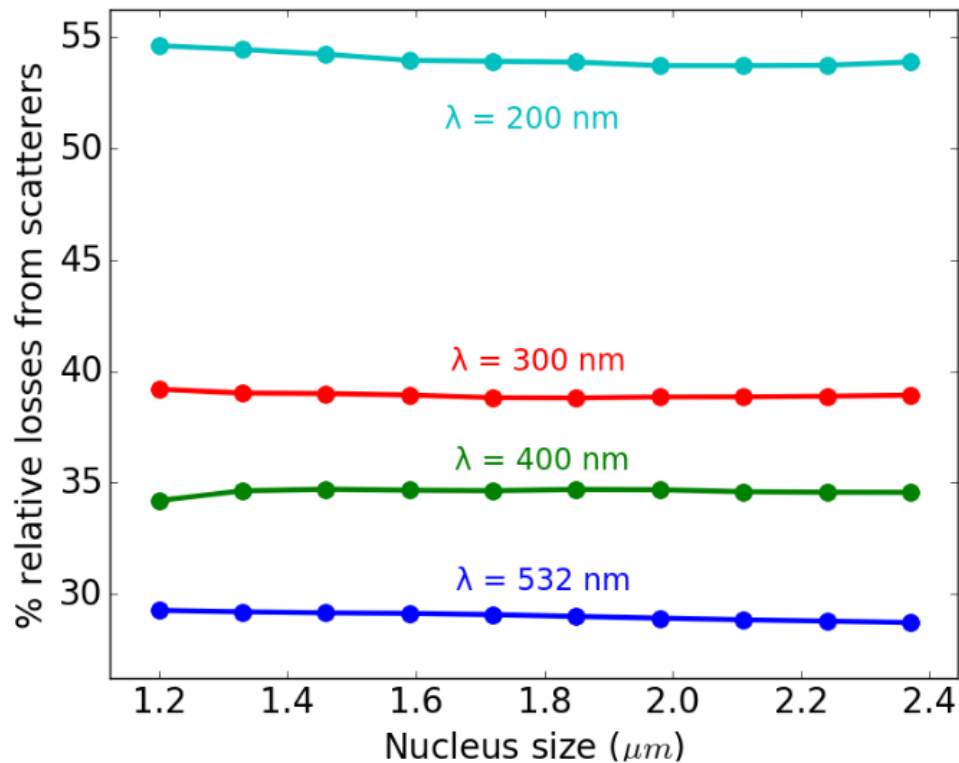
- both aspects of meas. bias demonstrated
- removed by intertwined measurements

1. class - noise correlation is broken in training set
2. training, validation and test sets do not share the same measurement conditions

# TRADE-OFF BETWEEN FIELD OF VIEW AND NUMBER OF SAMPLES

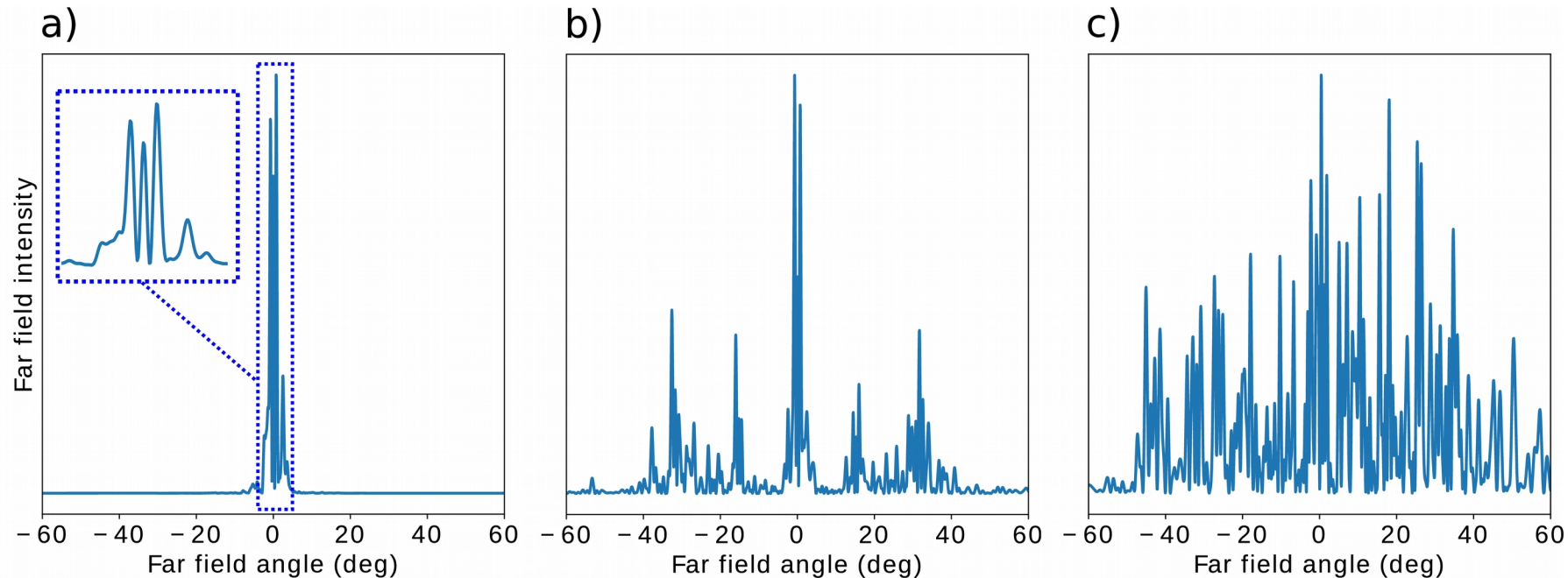


# RELATIVE LOSSES WITH 4 SCATTERING LAYERS



Relative to the case  
without scatterers

# INTENSITY IS MORE SPREAD OVER THE IMAGE SENSOR USING SCATTERERS

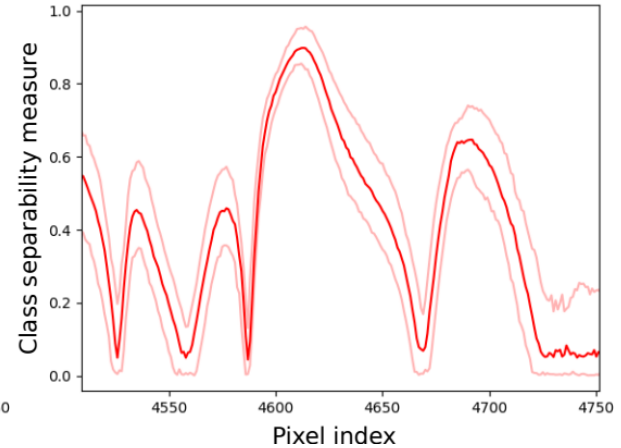
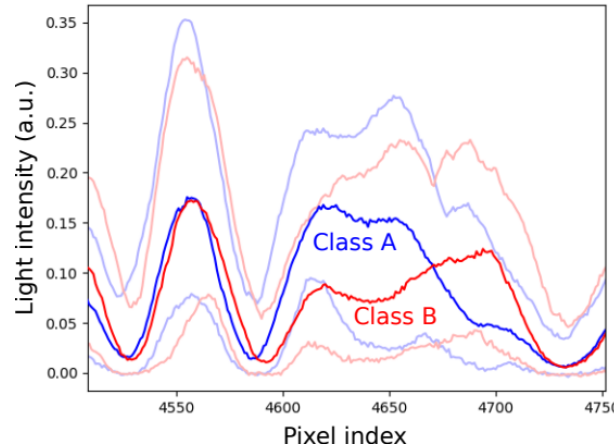


# MANN-WHITNEY U STATISTIC AND KENDALL CORRELATION

$$U = \sum_{i=1}^n \sum_{j=1}^m S(X_i, Y_j),$$

with

$$S(X, Y) = \begin{cases} 1, & \text{if } Y < X, \\ \frac{1}{2}, & \text{if } Y = X, \\ 0, & \text{if } Y > X. \end{cases}$$



Correlation calculated on pixel pairs

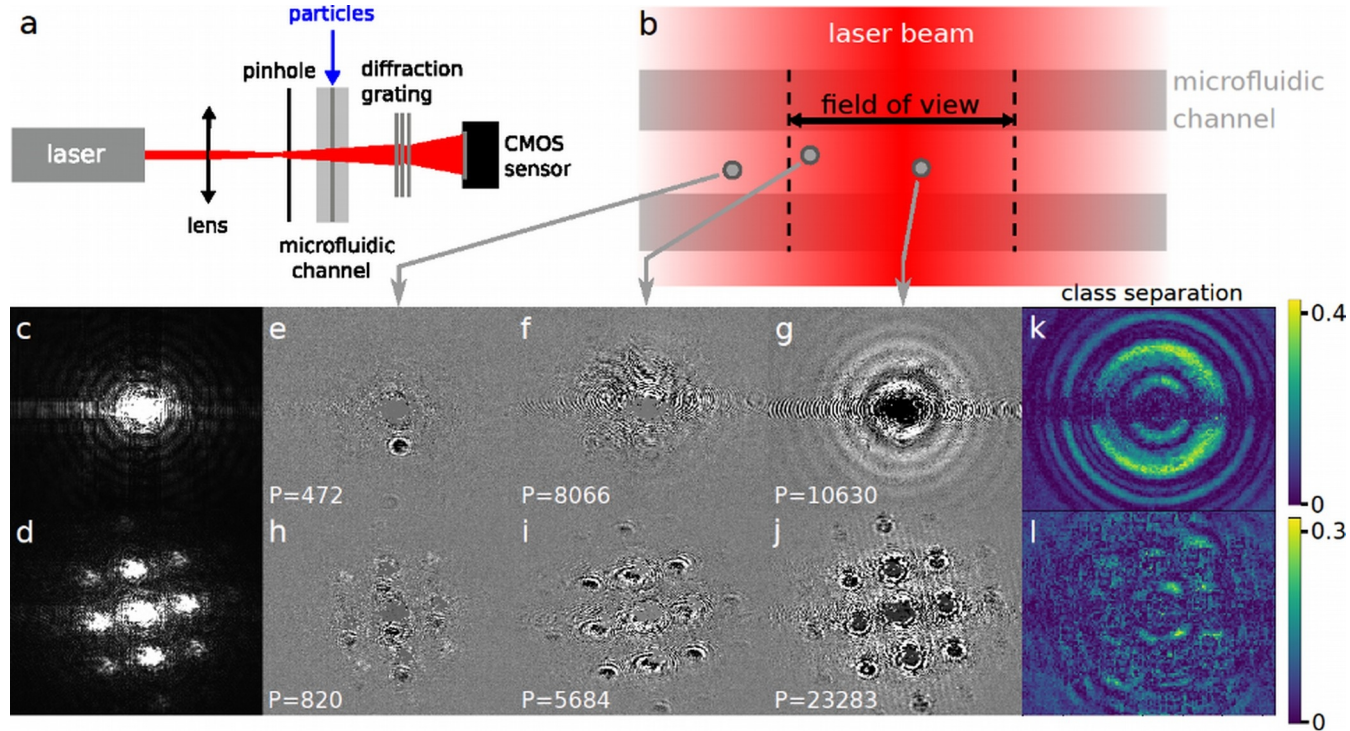
$$\tau_A = \frac{n_c - n_d}{n_0}$$

$$n_0 = n(n - 1)/2$$

$n_c$  = Number of concordant pairs

$n_d$  = Number of discordant pairs

# FIELD OF VIEW...



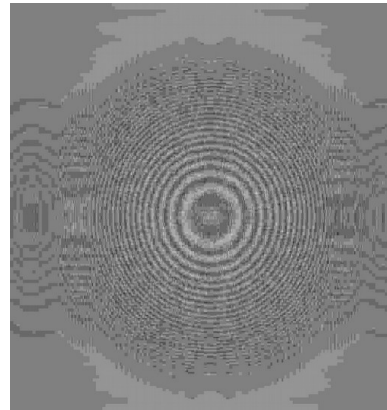
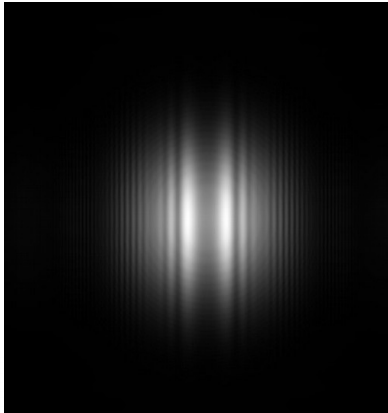
- Possible improvements:
- higher background-to-noise ratio
  - measure more samples
  - explore scattering configuration on morphology-based classification task (e.g. WBC)
  - partially automatized setup

# INTERFERENCE PATTERN

$$E(x, y, z) = \frac{e^{ikz}}{i\lambda z} e^{i\frac{\pi}{\lambda z}(x^2+y^2)} \mathcal{F} \left\{ E(x', y', 0) e^{i\frac{\pi}{\lambda z}(x'^2+y'^2)} \right\} \Bigg|_{p=\frac{x}{\lambda z}, q=\frac{y}{\lambda z}} \quad \text{Fresnel diffraction (near field)}$$

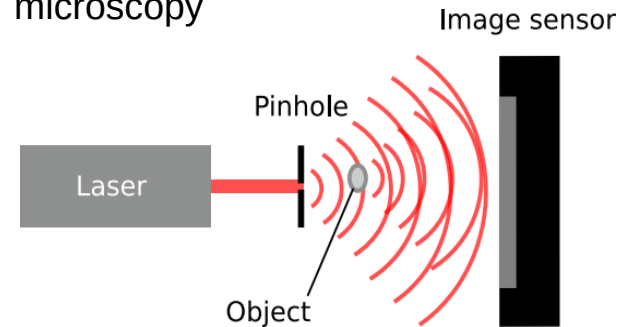
$$U(x, y, z) \propto \hat{f}[A(x', y')]_{f_x f_y} \quad \text{Fraunhofer diffraction (far field)}$$

Mie scattering is most suitable when the microparticle dimension is comparable with the wavelength

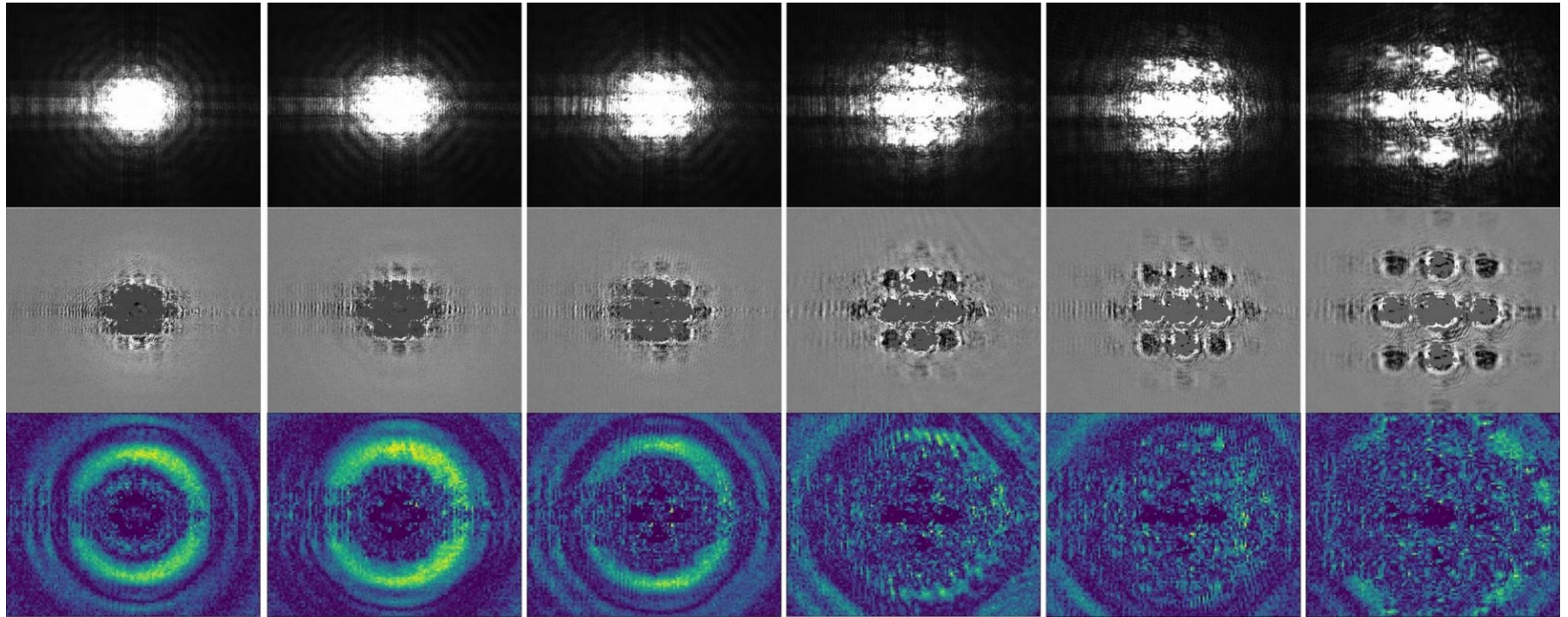


Emmanuel Gooskens  
UGent

Inline digital holographic  
microscopy



# DEPENDENCY ON CAMERA POSITION



# FOV ESTIMATION

from  $k$  particles in the FoV can be considered as the Poisson process describing the occurrence of  $k$  events  $t_{in}$ , with a time rate  $R_f$ , in a time interval  $\tau + \text{FoV}/v$ , with probability:

$$Pr(k, \tau + \text{FoV}/v, R_f) = \frac{[R_f(\tau + \text{FoV}/v)]^k}{k!} e^{-R_f(\tau + \text{FoV}/v)} \quad (5.4)$$

In our case  $\tau = 29 \mu\text{s}$  and we can calculate  $R_f$  by multiplying the flux rate (0.2 ml/min) by the estimated particle concentration, which depends on the particle class ( $1.6 \times 10^4$  and  $0.91 \times 10^4 \frac{\text{particles}}{\text{ml}}$  respectively for class A and B) since the mixtures have a common solid content volume. Note that we are assuming that the number of particles that remain stuck somewhere before reaching the illumination area is negligible w.r.t. the total number of passing particles. Therefore, even if we deem this assumption sufficiently true in our case, we should keep in mind that the estimated  $R_f$  is more an upper limit for the true particle flow rate. From the next calculation steps it will be evident that this implies that we will obtain a lower limit estimate of the true FoV. To provide an example calculation, assuming a reasonable FoV = 100  $\mu\text{m}$ , respectively for classes A and B we obtain (keeping 2 significant digits):  $Pr_A(k = 0) = 0.98$ ,  $Pr_B(k = 0) = 0.99$ ,  $Pr_A(k = 1) = 0.017$ ,  $Pr_B(k = 1) = 0.0098$ ,  $Pr_A(k = 2) = 0.00016$ ,  $Pr_B(k = 2) = 0.000048$ . These

through the microfluidic channel (statistical independence). The particle ratio  $R$  can be estimated by  $R = 1 - Pr(0, \tau + \text{FoV}/v, R_f)$ , with reference to equation (5.4). Thus, by inverting it, we can finally estimate the FoV corresponding to a chosen value of  $R$ :

$$\text{FoV} = -\frac{\ln(1 - R)v}{R_f} - \tau v \quad (5.5)$$

For each chosen value of  $R$  and for each particle class, we report in Table 5.3 the number of classification samples (accepted images) and the FoV estimates. The corresponding estimated FoV is quite large:  $\approx 0.3 \text{ mm}$ . It should also be stressed that, as a consequence of our choice of having a single threshold  $\theta_P$  for both classes and for training and testing, the FoV was class-dependent.

**No diffractive layer**

Particle rate	# accepted images		Field of view (mm)	
	class A	class B	class A	class B
0.02	1427	2108	0.09	0.25
0.04	4008	3067	0.27	0.37
0.06	6452	4120	0.45	0.51
0.08	7954	6051	0.56	0.76

Frame rate  $\sim 138 \text{ fps}$ , exposure time = 20  $\mu\text{s}$ ,  $\sim 5.5 \text{ p/s}$

# EXAMPLE ARTICLES

Lippeveld, Maxim, Carly Knill, Emma Ladlow, Andrew Fuller, Louise J. Michaelis, Yvan Saeys, Andrew Filby, and Daniel Peralta. "Classification of human white blood cells using machine learning for stain-free imaging flow cytometry." *Cytometry Part A* 97, no. 3 (2020)

- Proper ground truth with manual gating
- Deep learning does not outperform feature engineering
- 8 different types of WBC, but also 3 types classification
- Accuracy < 90%

Tang, Rui, Zunming Zhang, Xinyu Chen, Lauren Waller, Alex Ce Zhang, Jiajie Chen, Yuanyuan Han, Cheolhong An, Sung Hwan Cho, and Yu-Hwa Lo. "3D side-scattering imaging flow cytometer and convolutional neural network for label-free cell analysis." *APL Photonics* 5, no. 12 (2020)

- Label-free using light sheet and side scattering.
- 92% accuracy WBC classification
- Ground truth with manual gating